Design, Synthesis and Biological Evaluation of JNK1 Allosteric Inhibitors

A thesis submitted towards partial fulfillment of

5 year integrated BS-MS programme

by

Shishir Chourey

Under the guidance of

Dr Venkata Palle
Vice President
Lupin Limited, Pune

Dr Ramakrishna G. Bhat
Assistant Professor
IISER Pune

Department of Chemistry
Indian Institute of Science Education and Research, Pune
Maharashtra, India

IISER PUNE

भारतीय विज्ञान शिक्षा एवं अनुसंधान संस्थान, पुणे

INDIAN INSTITUTE OF SCIENCE EDUCATION AND RESEARCH (IISER) PUNE

900, NCL Innovation Park, Dr. Homi Bhabha Road, PUNE - 411 008.

CERTIFICATE

This is to certify that this dissertation entitled "**Design, Synthesis and Biological Evaluation of JNK1 Allosteric Inhibitors**" towards the partial fulfillment of the BS-MS dual degree programme at the Indian Institute of Science Education and Research Pune, represents original research carried out by Mr. **Shishir Chourey** at Novel Drug Discovery Centre, Lupin Limited (Research Park), Pune under the supervision of Dr Venkata Palle, Vice President during the academic year 2010-2011.

Institutional Supervisor

Dr. Ramakrishna G. Bhat

Assistant Professor, Chemistry

IISER Pune

Date:

Place:

Prof. K. N. Ganesh

Director and Head of Chemistry Dept

IISER Pune

Date:

Place:

CERTIFICATE

This is to certify that this dissertation entitled "**Design, Synthesis and Biological Evaluation of JNK1 Allosteric Inhibitors**" towards the partial fulfillment of the 5 year integrated BS-MS programme at the Indian Institute of Science Education and Research Pune, represents original research carried out by Shishir Chourey at Novel Drug Discovery and Development, Lupin Limited (Research Park), Pune under the supervision of Dr Venkata Palle, Vice President, Lupin Limited (Research Park), Pune.

Supervisor

Dr Venkata Palle

Vice President

Novel Drug Discovery Department

Lupin Limited (Research Park), Pune

Date:

Place:

CANDIDATE'S DECLRATION

I hereby declare that the matter embodied in the project report entitled **''Design, Synthesis and Biological Evaluation of JNK1 Allosteric Inhibitors''** is the result of investigations carried out by me at the at Novel Drug Discovery and Development, Lupin Limited (Research Park) under the supervision of Dr. Venkata Palle and submitted towards the partial fulfillment of the 5 year integrated BS-MS programme at the Indian Institute of Science Education and Research, Pune.

Shishir S. Chourey

Fifth year student

BS-MS dual degree program

IISER Pune

ACKNOWLEDGEMENT

I am grateful to Dr. Rajender Kamboj, Dr Venkata Palle and Dr Ramakrishna G. Bhat for providing an opportunity to do one year dissertation in the Novel Drug Discovery Department, Lupin Limited, Pune. With high regards and profound respect, I express my gratitude to Dr Bhavesh Dave, Dr Samiron Phukan and Dr. Mandar Bhonde who offered invaluable guidance, assistance and support. I express my deepest gratitude to the lab members; Jitendra Jadhav, Vikas Tambe and Gurpreet Kaur who were abundantly helpful, supporting and encouraging.

CONTENTS

ABSTRACT

c-Jun NH_2-terminal kinase (JNK) is a stress activated protein kinase which modulate cellular signaling that is implicated in a variety of diseases like type-2 diabetes, cancer, atherosclerosis, stroke, Alzheimer's and Parkinson diseases. JNK Interacting Protein 1 (JIP1) is a scaffolding protein of JNK which enhances JNK signaling by integrating the modules of JNK signaling. A part of the scaffolding protein- JIP-1 containing 153- 163 AA residues - known as pepJIP1 acts as an inhibitor to JNK at an allosteric site. The present work aims in design, synthesis and biological activity of small molecule allosteric inhibitors of JNK1.

LIST OF FIGURES

LIST OF TABLES

LIST OF SCHEMES

ABBREVIATIONS

AA- Amino acid

AP1- Activator Protein 1

ATF2- Activating Factor 2

ATP- Adenosine Tri Phosphate

DCM- Dichloromethane

DIPEA- N,N-Diisopropylethylamine

DNA- Deoxy RiboNucleic Acid

ED- Extracellular Domain

EDCI- 1-Ethyl-3-(3-Dimethylaminopropyl)carbodiimide

GPCR- G-Protein Coupled Receptors

HATU- 2-(1H-7-Azabenzotriazol-1-yl)--1,1,3,3-tetramethyl uronium hexafluorophosphate Methanaminium

HOBT- N-Hydroxybenzotriazole

HPLC- High Performance Liquid Chromatography

ITAM- Immunoreceptor Tyrosine-based Activation Motif

mRNA- Messenger RiboNucleic Acid

NMM- N-Methylmorpholine

NMR- Nuclear Magnetic Resonance

RMSD- Root Mean Square Deviation

SH2- Src Homology 2

TFA- Trifluoroacetic acid

TNF- Tumor Necrosis Factor

UV- Ultraviolet

1. INTRODUCTION

1.1. Protein Kinase

1.1.1. The Kinome

The kinome is the set of genome compliments to protein kinases. The human kinome comprises 2% of its genome; consisting 518 protein kinases [1]. Protein kinases are enzymes which catalyze the transfer of the γ-phosphate group of ATP to their protein substrates (Figure 1.A). On the other hand, phosphatases are enzymes which remove the phosphate group from the proteins. The phosphorylation of a protein by a protein kinase can either increase or decrease the protein's activity, depending on the site of phosphorylation and the structure of the protein (Figure 1.B). During phosphorylation the structure of protein is modified which lead to the change in protein activity. Thus protein kinases are key regulators of cell signaling and functioning [2].

1.1.2. Influence of protein phosphorylation on protein activity

In late 1970's it became clear that proteins are not post-translationally modified merely by glycosylation but might be reversible modified as a response to external as well as internal stimuli [2]. Protein phosphorylation is one of the methods for reversible and regulatory modification of protein. It controls the protein function through the covalent addition of a phosphate group to the amino acid side chains of protein substrates.

In the process of phosphorylation, protein is structurally modified which affects its function in two important ways. First, because each phosphate group carries two negative charges, binding of a phosphate group to a protein can cause major conformational changes by attracting a cluster of positively charged amino acid side chains (Figure 2). This in turn affects the binding of ligands to the protein by revealing the binding sites on the protein surface which were concealed otherwise. And the binding of ligands to the revealed sites upon phosphorylation dramatically changes the protein activity. And when the phosphate group is removed, the protein returns to its original confirmation restoring its activity. Second, an attached phosphate group can form part of

a structure that the binding sites of other proteins recognize. For example, SH2 domain binds to a short peptide sequence containing phosphorylated tyrosine side chains.

Protein phosphorylation and dephosphorylation drive the regulation of assembly and disassembly of protein complexes. That is how reversible protein phosphorylation controls the protein conformation and activity.

1.1.3. Structural Elements of Protein Kinase

Comparative analysis of amino acid sequence of the members of protein kinase family shows that they share a sequentially and structurally homologues domain of 250-300 amino acids called as catalytic domain [5]. This catalytic domain is further classified into 11 conserved subdomains and folded into two lobes. One of the two lobes is a smaller NH_2-terminal lobe which contains a glycine rich loop (P-loop) for ATP binding. The second one is CO_2H- terminal domain, with a conserved activation loop (T-loop), which itself is regulated phosphorylation (Figure 3) [6].

1.1.4. Classification of Protein Kinases

The eukaryotic protein kinases superfamily is divided into distinct families based on their structural and functional properties (Figure 4). Comparison of the amino acid sequences at the catalytic domain of kinases has been extensively used to place them in evolutionary tree [7]. Different kinases having structurally closed catalytic domain also have similar overall structure, substrates and modes of regulation. This classification scheme became indispensible in the analysis of protein kinases as more and more sequence information became available as a consequence of genome projects [8].

1.1.5. Protein Kinases- the major drug targets of the twenty-first century

Protein Kinases are versatile and complicated proteins which control the complex cellular signaling networks. Interplay of activation and inhibition of protein kinases produces a variety of cellular responses, tweaking a precise cell behavior [9]. For such a robust signaling network a tight regulation of the kinase activity is required as it is linked to several cellular processes like cell metabolism, transcription, cytoskeleton rearrangement and cell movement, cell cycle

progression, cell differentiation, apoptosis, physiological responses, homeostasis and function of the immune system [10].

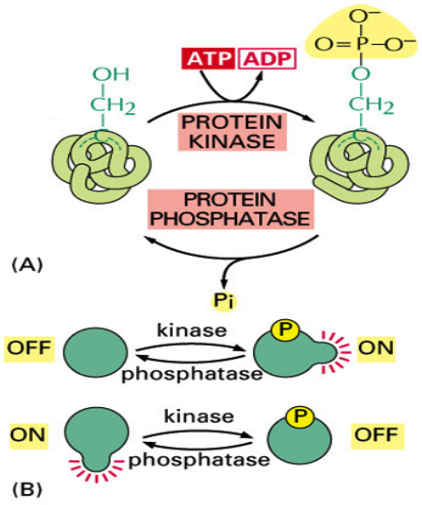

Figure 1| Schematic representation of protein phosphorylation [3]

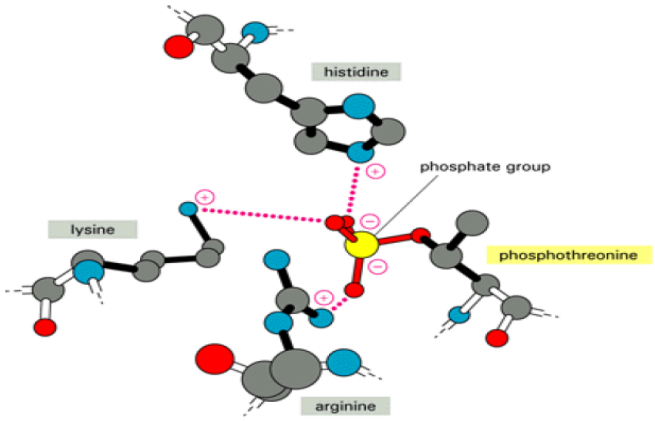

Figure 2| The influence of a phosphate group on a protein

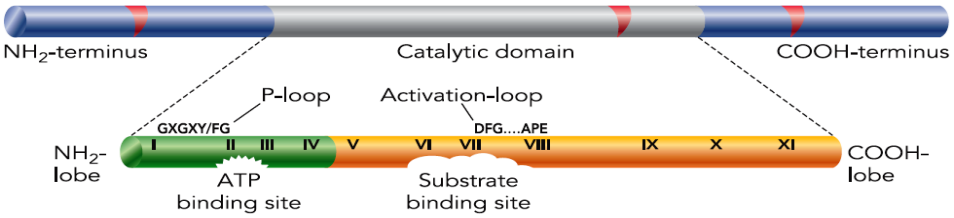

Figure 3| Representation of structural domain of protein kinase [4]

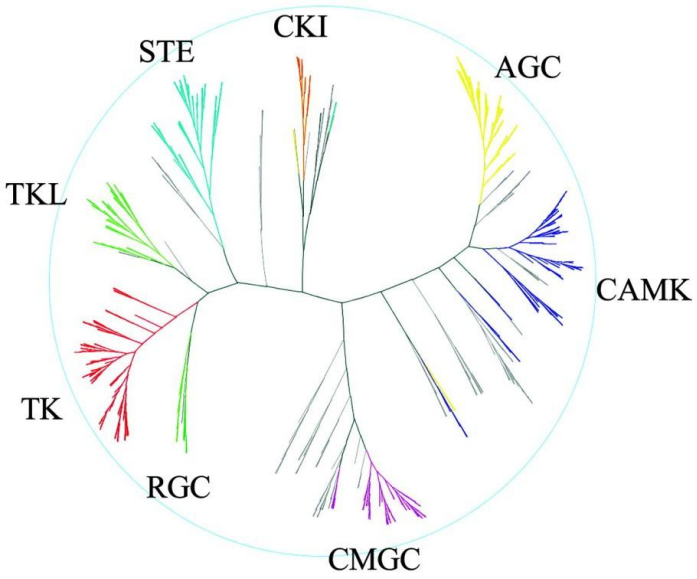

Figure 4| Dendogram of the human protein kinase superfamily [8]

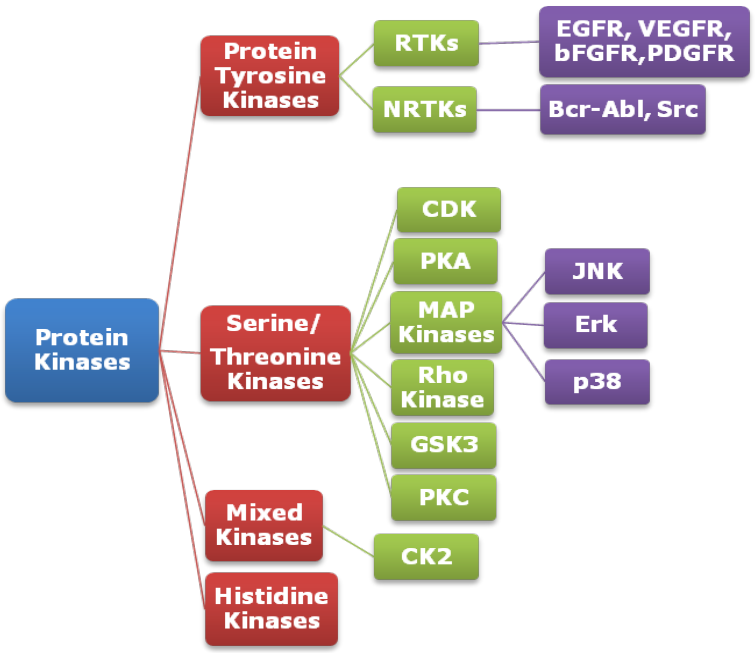

Figure 5| Hierarchy of protein kinases inferred from their catalytic substrate

A perturbation of kinase activity (i.e. abnormal phosphorylation) is a cause or consequence of diseases (Cancer, diabetes, inflammation etc.) [10]. Protein kinases have now become the second most important group target after GPCR. So there has been a growing interest in the development of protein kinase inhibitors in the quest of new therapeutics [11].

1.1.6. Protein Kinase Inhibitors

Since many protein kinases have been implicated in the key steps of cellular processes like differentiation and apoptosis, the discovery of small molecule kinase inhibitors has fascinated emerging interest for the development of novel drugs as well as understand the biological roles of kinases. The protein kinase inhibitors can be classified into different types based on their binding site and conformation of the target kinase [12].

Type I inhibitors:

Small molecule inhibitors targeting the ATP binding site of the enzyme in the active form are defined as Type I inhibitors. They bind the enzyme in a catalytically active DFG “in” conformation which is an open conformation of the kinase based on the position of the conserved triad Aspartate-Phenylalanine-Glycine (DFG) at the beginning of the activation loop (Figure 6). These compounds mimic the interactions of the adenine ring of ATP and binds to the “hinge” region of the protein kinase by forming hydrogen bonds.

Type II inhibitors:

They bind to inactive kinase form that is characterized by DFG “out” form and stabilize it. The DFG “out” form leads to the opening of an additional cavity, the allosteric site which is hydrophobic in nature which is specifically targeted by these compounds. So type II inhibitors not only bind the ATP binding site but also exploit the hydrophobic interactions within the allosteric site which offer some advantages in terms of selectivity compared to Type I inhibitors.

Type I½ inhibitors:

These compounds bind to the adenine region like Type II inhibitors forming hydrogen bonds with the hinge region and then extend into the hydrophobic back cavity of the ATP site. Thus,

following this class of compounds it is possible to target a DFG “in” motif with type II allosteric interactions which is a characteristic of a DFG “out” form.

1.1.7. Mitogen Activated Protein Kinases

Activation and signaling

The mitogen-activated protein kinases (MAPKs) are a family of serine/threonine kinases that play an essential role in signal transduction by modulating cellular activities in response to the extracellular stimuli (Figure 7). MAPKs control many physiological processes, including proliferation, differentiation and apoptosis; also participate in a number of disease states including chronic inflammation and cancer. They include the extracellular signal-regulated protein kinases (ERK1 and ERK2); c-Jun N-terminal kinases (JNK1, JNK2, JNK3); p38’s (p38a, p38b, p38c, p38d) and ERK5. MAPKs are activated by signaling cascade modules which consist of the upstream kinases of MAPKs, MAPK kinases (MKKs) and the upstream kinases of MKKs, MAPK kinase kinases (MKKKs) [13].

Scaffolding Proteins

The diverse combination of MAPK, MAPKK, and MAPKKK seems to cause the extreme complexity in the cellular response to a wide range of stimuli. The specificity of MAPK signal transduction is achieved by the use of scaffolding proteins which coordinate the interaction of the three components of the MAPK cascade by phosphorylation and protein-protein interaction. Scaffolding proteins assemble the units or modules of MAPK signaling that are responsive to particular stimuli and therefore obtain the appropriate cellular target by being insulated from similar units (Figure 8) [13].

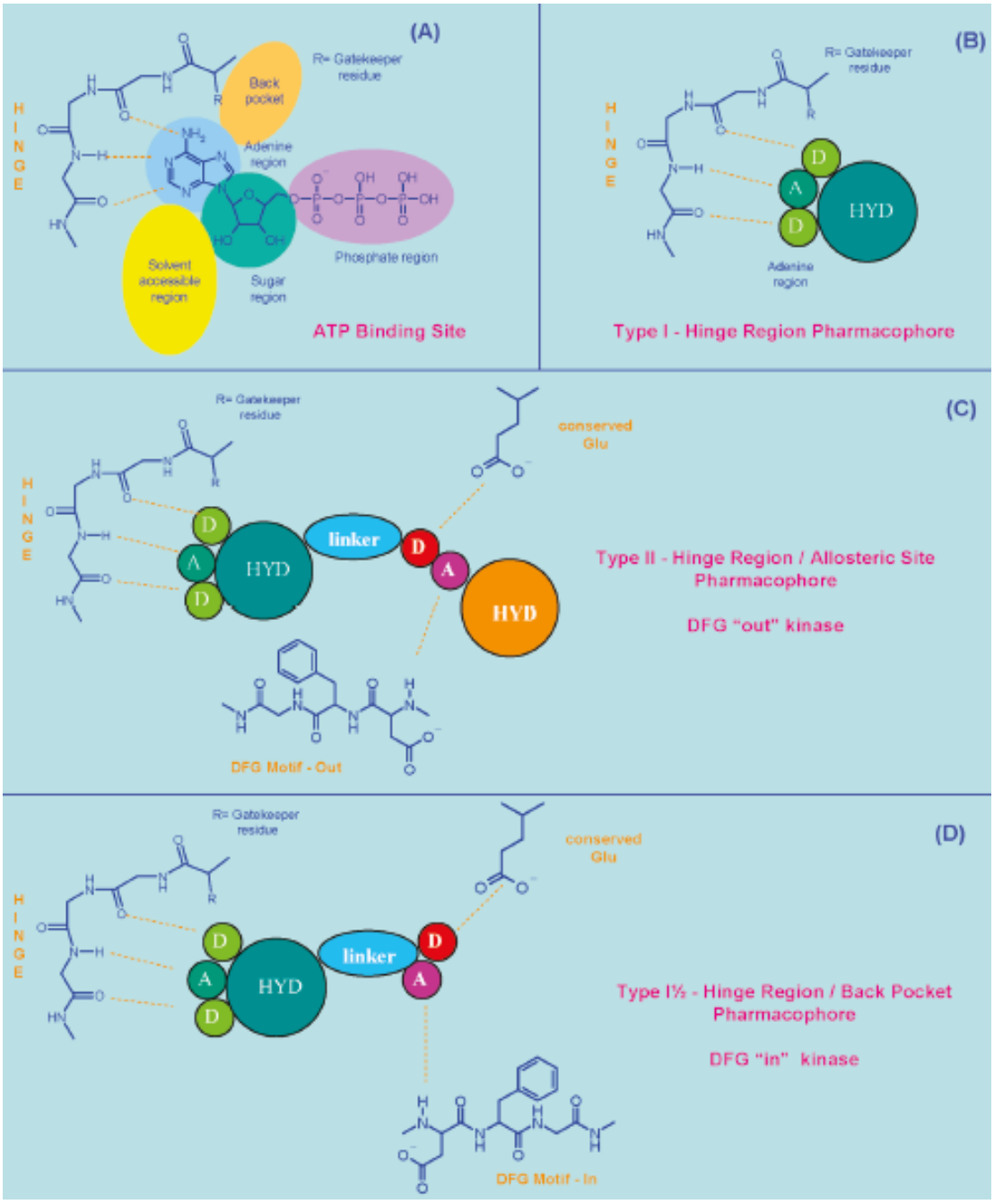

Figure 6| Classification of protein kinase inhibitors [12].

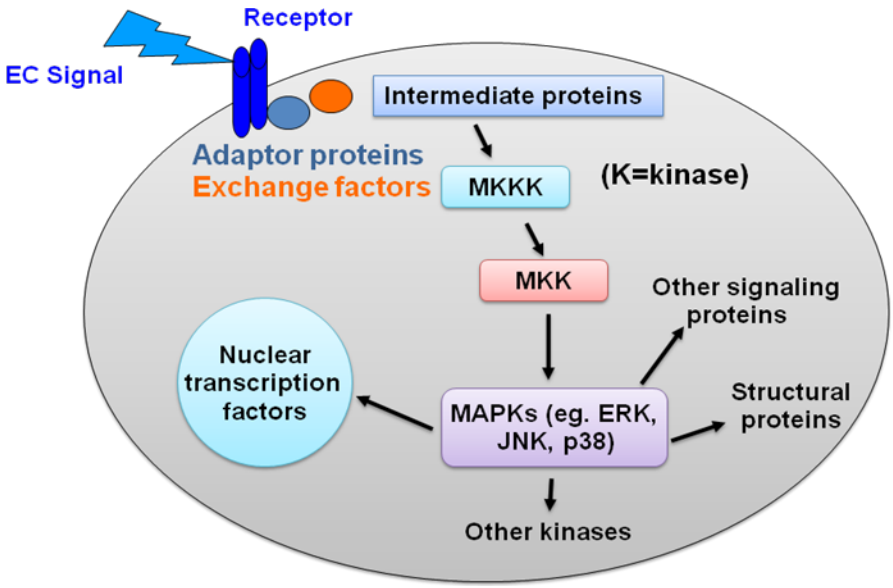

Figure 7| Integration of the MAPK pathway in the cellular response to environmental stimuli

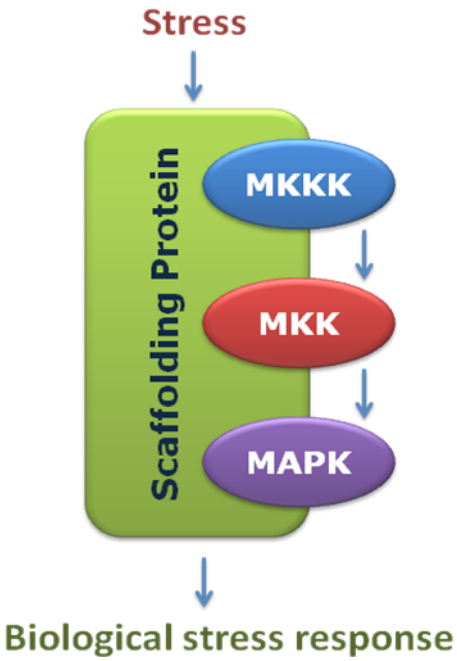

Figure 8| MAP-kinase-scaffold complexes.

1.2. c-Jun NH_2-terminal Kinase1 (JNK1)

1.2.1. The JNK family

JNKs are members of the Mitogen Activated Protein Kinase (MAPK) family that are activated by stress stimuli like UV radiation, cytokines and environmental stress hence also called as Stress Activated Protein Kinase (SAPK). JNK was first isolated and purified in 1990 by Kyriakis *et al*. as a protein kinase that was activated in the liver of rodents exposed to cycloheximide [15]. JNKs are encoded by three alternatively spliced genes *Jnk1*, *Jnk2* and *Jnk3*. Alternative splicing of mRNA transcripts derived from these genes result ten JNK isoforms. JNK1 and JNK2 are widely expressed in a variety of tissues while the expression of JNK3 is restricted to the brain, heart, pancreatic islet cells and testes [16].

1.2.2. Activation and Signaling

JNK is activated by dual phosphorylation of the Thr-Pro-Tyr motif located in the activation loop [17] and inactivated by Ser/Tyr phosphatases as well as dual specificity MAPK phosphatases [18]. Once activated, JNK phosphorylate several transcription factors, and cellular substrates which are responsible for cell proliferation, insulin receptor signaling, mRNA stabilization and apoptosis. JNK is essential for TNF-α induced c-Jun phosphorylation and AP-1 transcription factor activity. Phosphorylated AP-1 develop an enhanced DNA binding ability and transcription activity [19].

JNK-interacting protein (JIP1) is a scaffolding protein of the JNK consists of the three different modules (components); JNK, upstream kinase of JNK (MKK7) and upstream kinase of MKK7 (MLK). JIP1 enhances JNK signaling by creating proximity effect between JNK and its upstream kinases. Together these protein Kinases are capable of forming signaling cascades which response to specific stimuli by mediating JNK activation [14].

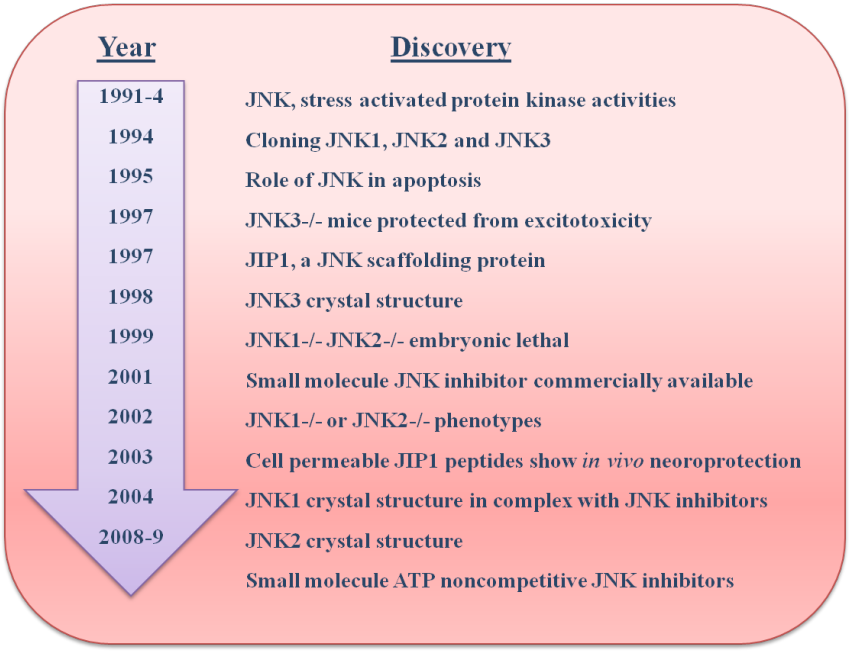

Figure 9| Landmark discoveries in the area of JNK research [20]

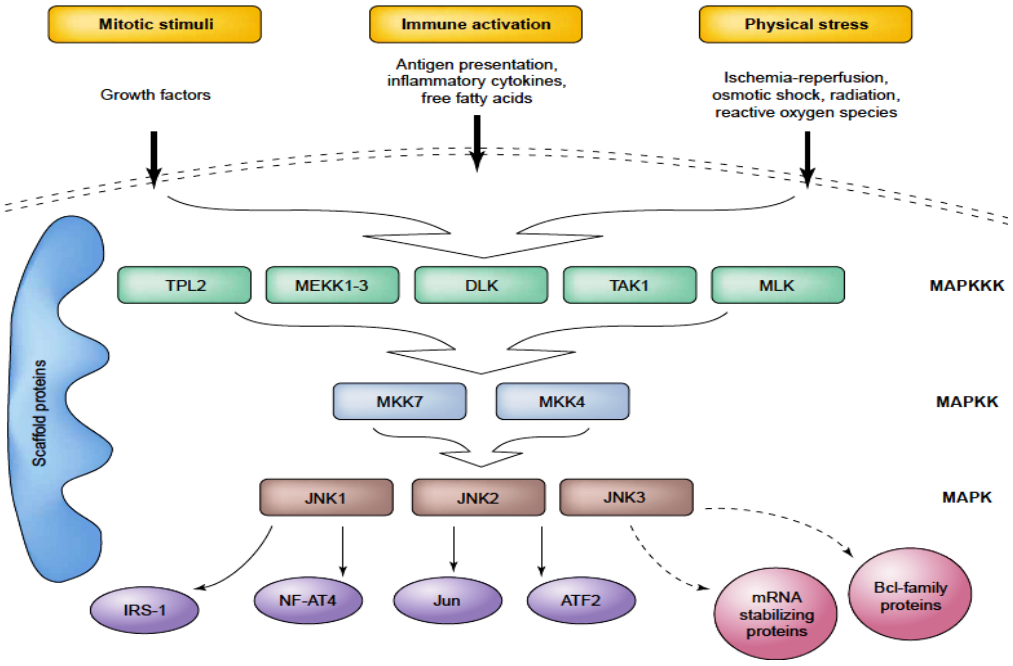

Figure 10| The JNK signaling pathway [21]

1.2.3. Targeting JNK for therapeutic benefit

JNK plays a pivotal role in metabolic conditions such as obesity, inflammation, insulin resistance and type-2 diabetes [19]. The improved understanding of JNK structure, regulation and function made it possible to develop JNK inhibitors that have therapeutic impact [22].

Role of JNK1 in insulin sensitivity and Cancer

Insulin Receptor Substrates (IRS) are key regulatory proteins that are phosphorylated on multiple (>30) tyrosine residues. When insulin molecule binds to IRS, a phosphorylation cascade is initiated that promotes the effects of insulin in the cell [23]. However, failure to activation of IRS results in insulin resistance. It is a physiological condition in which Insulin becomes less effective in lowering blood glucose level. Although tyrosine phosphorylation activates IRS, selective serine phosphorylation can inactivate or downregulate IRS. It contains a docking site for the binding of JNK. It is been identified that IRS1 Ser307 is an important site for TNF-α induced phosphorylation by JNK. It is evident from the fact that insulin stimulated IRS1 Ser307 phosphorylation was inhibited in cells lacking JNK and also in cells expressing a mutant IRS1 lacking the JNK binding domain. Also it was observed that there is a loss of Ser307 phosphorylation in case of *Jnk1-/- ob/ob* mice [24].

Based on the above facts it is proposed that in case of obesity there is an elevated level of TNF-α and FFA which directly activate JNK as a stress response [25]. This in turn inactivates IRS and inhibits the action of insulin, promoting insulin resistance which indicates that JNK is an important negative feedback regulator of insulin signaling. Therefore JNK1 inhibitors would be quite useful for improving insulin resistance and hence reducing the risk of type-2 diabetes [22].
The JNKs are implicated in several physiologic processes, including proliferation, apoptosis, and differentiation. Although JNK1 or JNK2 mutations are not prevalent in cancer, many tumor cell lines have been reported to possess constitutively active JNKs. The expression of JNK1 was markedly increased in breast cancer tissue compared with normal samples. Recent studies from Chen's laboratory also indicated that JNK1 played a pivotal role in the expression of the key signature genes and the prognostic outcomes of human hepatocellular carcinoma. The molecular mechanisms underlying the oncogenic role of JNK1 need to be further exploited [42].

1.2.4. JNK Inhibitors

JNKs are being targeted in the quest of new therapeutics and to understand their physiological roles at a bigger domain [26]. All known JNK inhibitors are generally small molecules which compete with ATP molecules for binding to ATP binding site on JNK (Figure 12). Due to the high structural similarities of ATP binding site of all MAPK (e.g. p38 and Erk) there is a need to develop selective inhibitors of JNK [27]. Thus ATP non-competitive (allosteric) inhibitors of JNK1 have attracted growing interest.

pepJIP1 as an allosteric inhibitor of JNK1

The JNK1- JIP1 interaction is mediated by a high affinity and specific D-domain on JIP1. Overexpression of either the single D-domain or full length protein (JIP1) inhibits JNK1 signaling in the cell [28]. The single D-domain of JIP1 consisting an 11-mer docking site peptide (residues 153- 163) has been identified as a JNK1 inhibitor, known as pepJIP1 [29]. The pepJIP1 binds to the docking grove of JNK1 which is away from the ATP pocket or substrate recognition site, implying that pepJIP1 acts as an allosteric inhibitor of JNK1 [30]. The mechanism of JNK1 inhibition by pepJIP1 is described below:

i. The binding of pepJIP1 to JNK1 leads to the cytoplasmic retention of JNK1 and therefore inhibits the gene expression mediated by JNK1, which occurs in the nucleus [30].
ii. PepJIP1 competes for binding with the D-domains of JNK substrates (ATF2) or upstream kinases of JNK [31].
iii. Binding of pepJIP1 induces a hinge motion between the N- and C-terminal domains of JNK1 and distorts the ATP-binding cleft, reducing the affinity of JNK1 for ATP [30].

However poor cell permeability, peptide instability and short half-life *in vivo* of pepJIP1 restrict the development of peptide-based inhibitors but facilitate the development of small molecules mimicking pepJIP1 as inhibitors of JNK1 [31].

Therapeutic promise of small molecule allosteric inhibitors of JNK1

JNK1 phosphorylation is mediated through the protein- protein interaction with JIP1. Blocking the docking grove of JNK1 with small molecules prevents the JNK1- JIP1 interaction and subsequent phosphorylation of JNK1 [31]. The pepJIP1 would be an excellent scaffold to design such molecules since it is an inhibitor of JNK1 and 3D- structural information on JNK1- pepJIP1 interaction is available [26]. Moreover the challenge of designing small molecules inhibitors of kinases as ATP competitive specific to a particular target could be mitigated by this allosteric site.

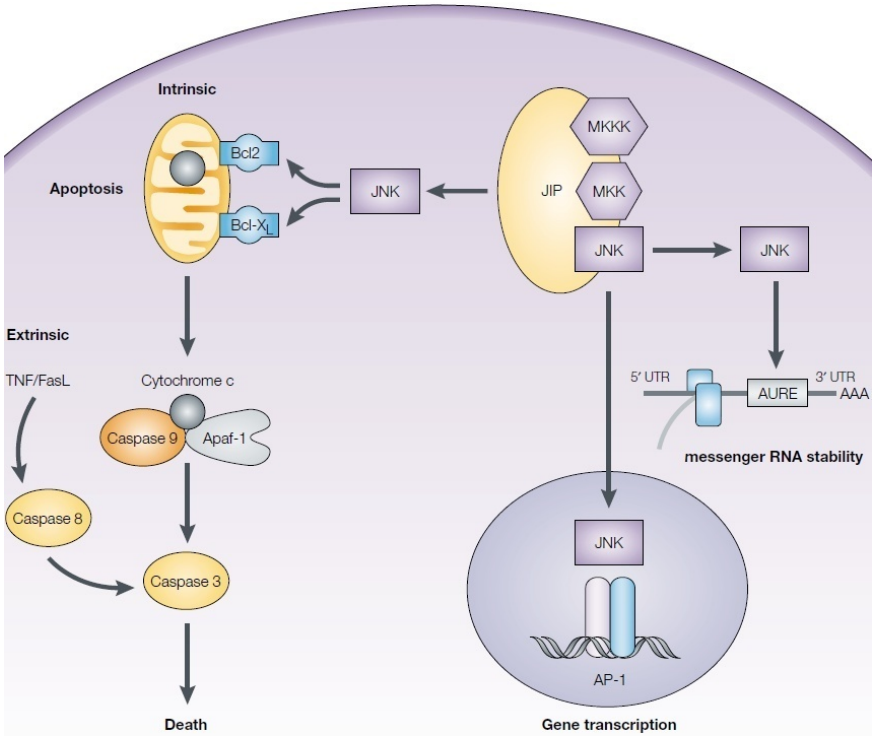

Figure 11| Biological functions of JNK [32]

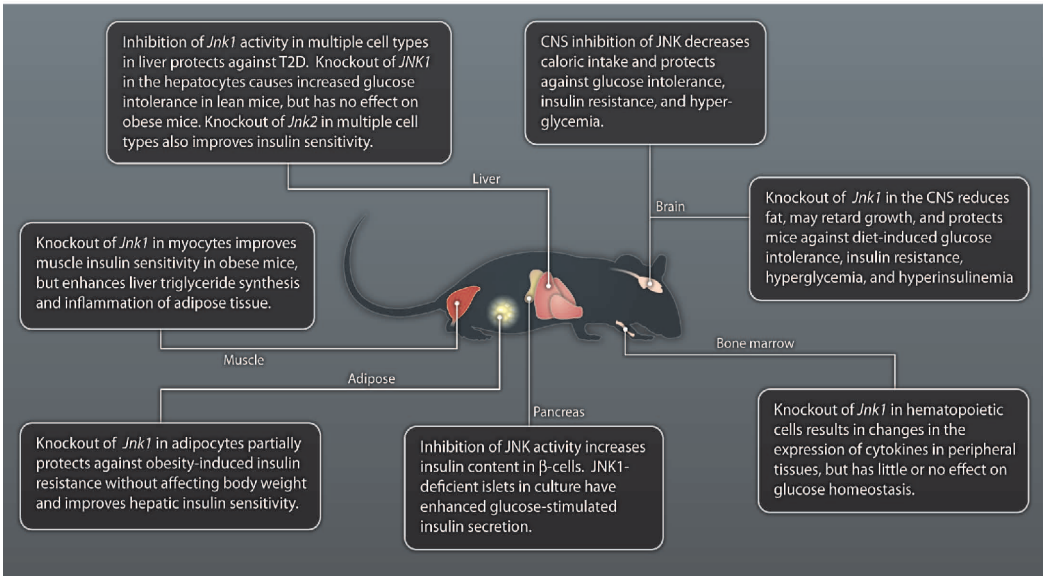

Figure 12| Targeting JNK in different tissues [22]

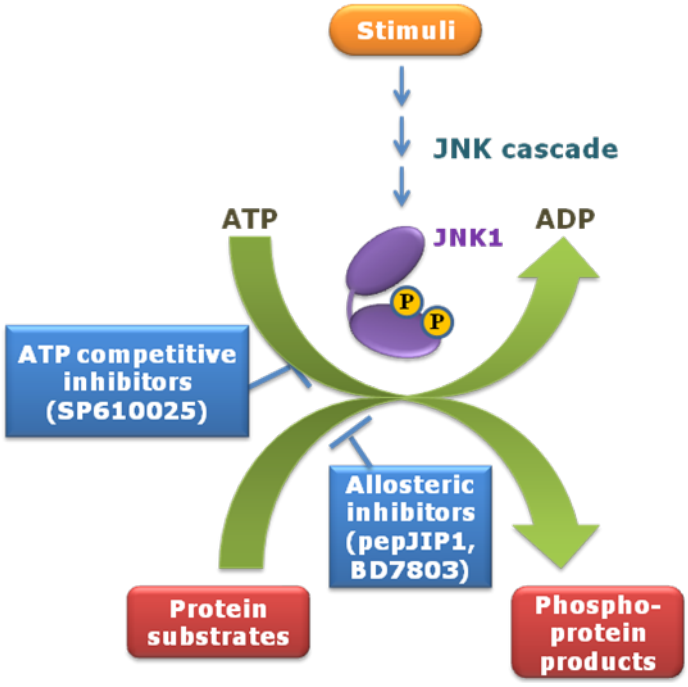

Figure 13| JNK1 inhibitors

1.3. Objectives of the project:

This project was carried out with the following objectives.

i. Structural analysis of competitive and non-competitive inhibitors of JNK1.
ii. Crystal structure analysis of pepJIP1- JNK1 complex.
iii. Design of compounds as allosteric inhibitors of JNK1.
iv. Synthesis of designed compounds.
v. Biological evaluation of synthesized compounds.

2. METHODOLOGY

2.1. Molecular Modeling

2.1.1. Crystal structure Analysis of JNK1

There are eight crystal structures of JNK1 available on the Protein Data Bank (PDB) [34]. The structures varied from 1.8 to 3.5Å in resolution. The structures were analyzed with respect to their both binding sites (ATP binding and allosteric binding). The allosteric binding site is the site where the pepJIP1 binds to JNK1. After analyzing the structural features of the crystal structures 1UKI (resolution- 2.7Å) was chosen as the template structure due to the availability of the 11-mer peptide from C-jun-amino terminal kinase interacting protein1 (pepJIP1) bound to it and the presence of co-crystallized small molecule JNK inhibitor (SP600125) at the ATP binding site.

2.1.2. Docking studies of reported JNK1 allosteric inhibitor

Binding modes for the interaction of pepJIP1 to JNK1 were evaluated in order to identify the crucial residues for this stable protein-protein interaction. These critical residues for protein-protein interaction are also called as hot spots. Identification and evaluation of the hot spots for binding of pepJIP1 to JNK1 was carried out by analyzing the crystal structure of pepJIP1-JNK1 complex. To this site the reported JNK1 small molecule allosteric inhibitors were docked to understand the probable binding modes. The result of this docking study is tabulated in table 1 (supporting information). The docking study was done using the docking tools like Glide [34] (Schrodinger), Surflex-dock [35] (Sybyl) and Grip dock [36] (MDSV-life). Each of the docking modules works on different algorithms and adheres to different docking protocols which are described below.

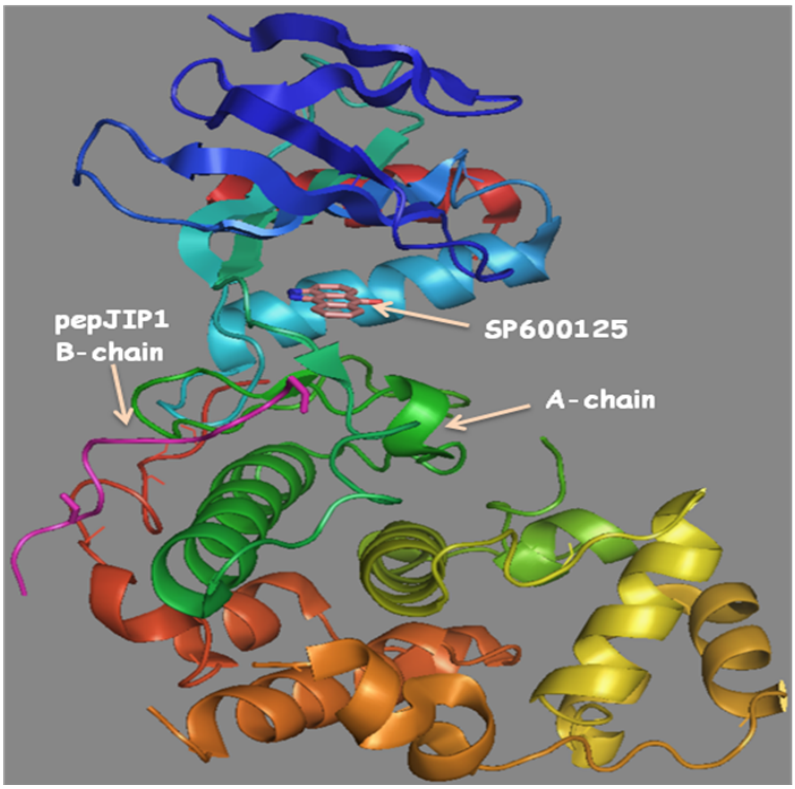

Figure 14| Crystal structure of JNK1 (PDB ID- 1UKI)

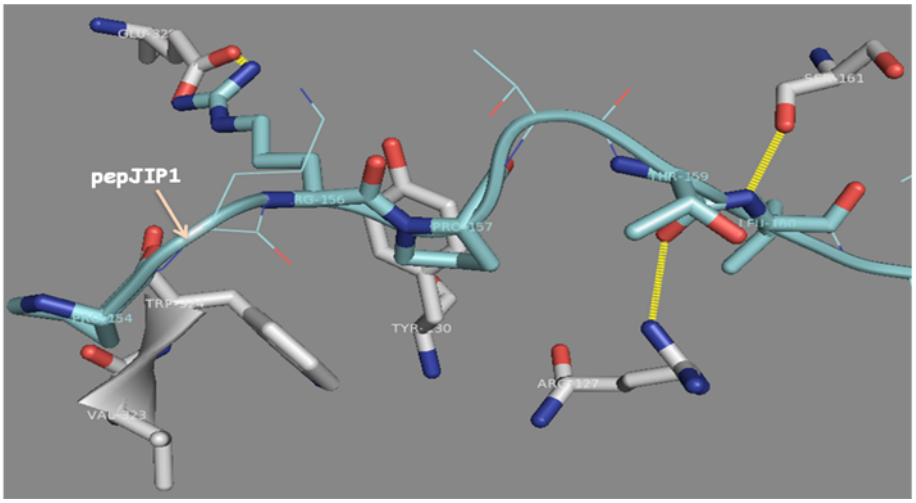

Figure 15| Prominent interactions in the pepJIP1-JNK1 complex

GLIDE (Schrodinger)

Ligand Preparation:

The three-dimensional structures of 49 known small molecules JNK1 inhibitors were prepared using the LigPrep module of Maestro v7.0.113 in the Schrödinger suite of tools19. The bond orders of these ligands were fixed and the ligands 'cleaned' through LigPrep specifying a pH value of 7.0. All the tautomers of the compounds were chosen. In the final stage of LigPrep, the compounds were energy minimized by using the force field OPLS2005 [37].

Protein Preparation:

Out of eight PDB structures (available at the time of study) 1UKI was chosen for the docking studies. This was taken due to the availability of allosteric binding sites. All the crystallographic water molecules deleted and hydrogens were added to the X-ray structure of the protein. The guanidines and ammonium groups in all the arginine and lysine side chains were made cationic and the carboxylates of aspartate and glutamate residues were made anionic. Following these steps, the X-ray structure was subjected to the energy minimization using the Schrödinger implementation of OPLS-2005 force field with implicit salvation [37].

Docking:

Docking studies on LigPrep-treated actives were carried out in the pepJIP1 binding site of JNK1 using the Schrodinger docking program, Glide. The protein–ligand complexes prepared as described above were employed to build docking grids using the default value of protein atom scaling (1.0) within a cubic box of dimensions 30 Å × 30 Å × 30 Å centred around the centroid of the X-ray ligand pose. The bounding box (within which the centroid of a docked pose is confined) dimensions were set to 10Å × 10 Å ×10 Å. The best docked pose (with highest GlideScore value) was saved per ligand. The representative results of XP docking scores are provided in table 1 (supporting information).

Surflex Dock (SYBYL)

Protein Preparation:

One out of eight PDB structures (available at the time of study) was chosen for the docking studies, (PDB ID- 1UKI). Using the docking suite pepJIP1 was extracted and set as a protomol. The resulting structure was then prepared by adding hydrogens, fixing sidechains amide and minimizing the energy. The lowest energy was set to 0.05 kcal/mol which was achieved by 100 gradient iterations using the method “Powell”, force field “Tripos” [38], NB Cutoff- 8.0 and LS step size- 0.001.

Ligand Preparation:

The structures of 49 small molecules JNK1allosteric inhibitors were imported as sd files. The three-dimensional structures these molecules were prepared using the Ligand Preparation module of SYBYL-X 1.2 (Tripos). The module requires all input molecules be protonated at physiological pH including non-polar hydrogens. For all the ligands, lowest strain energy tautomers/stereoisomers were generated by the “custom” protocol and the energy minimization was done with Merck Molecular Force Field (MMFF) [39].

Docking:

Docking studies on the prepared ligands were carried out in the pepJIP1 binding site of JNK1 using the Sybyl (Tripos) docking suite, Surflex-Dock 2.1. A protomol was generated around the JIP binding site by selecting all the residues with the selection radius of 3Ǻ around pepJIP1. In surflex docking, 3D coordinates (concord) were generated wherever necessary. Maximum conformations per fragments andǺ to expand search grid were set to 20 and 6 respectively. Soft Grid treatment was used and the protein-ligand pairs were relaxed. Spin alignment method was activated in which the density of search was set to 3.0 and the numbers of spins per alignment were restricted to 12. Following these, consensus scores (CScores) were generated. In output options maximum numbers of poses per ligand were allowed to 20 and the minimum RMSD between the final poses was 0.05. The corresponding CScores are given in table 1 (supporting information).

Grip dock (VLifeMDS3.5)

Protein Preparation:

As mentioned earlier in the previous two softwares, 1UKI was taken for docking studies using VLifeMDS3.5. PepJIP1 and all the crystallographic water molecules were deleted. Following these steps, the X-ray structure was subjected to the optimization using Merck Molecular Force Field (MMFF) and "Gasteiger-Marsil" charges [40]. For optimization RMS gradient (analytical) and maximum number of cycles were set to 0.01 and 10000 respectively.

Ligand Preparation:

The three-dimensional structures of 49 reported small molecules JNK1 inhibitors were optimized using the Biopredicta module of VLifeMDS3.5. The input molecules were energy minimized with Merck Molecular Force Field (MMFF). The conformers of the input molecules were generated by using the 'systemic' method in which the total number of rotatable bonds per molecule was restricted to five. All the generated conformers were chosen for the further studies.

Docking:

Docking studies on prepared ligands were carried out in the pepJIP1 binding site of JNK1 using the VLifeMDS3.5 docking program, GRIP docking. Chain B was chosen as a reference ligand around which the grid was generated. Then chose parameters as 'Exhaustive' and input Rotation Angle step size of 30° by which the ligand was rotated for different poses. Maximum number of placements per ligand was restricted to 30. The corresponding docking scores are given in table 1 (supporting information).

2.1.3. Design of Allosteric inhibitors

NCE's were designed targeting the hot spots of JNK1 which maintains the binding of pepJIP1. The main hypotheses for design of NCE's were:

i. Geometry mimic of the allosteric site
ii. Engagement of critical residue interaction with JNK1 (Arg127 and Glu329).

Based on the above criterion peptide scaffolds were designed which can potentially mimic pepJIP1 and bind effectively to JNK1, thus inhibiting JNK1-pepJIP1 interaction. All the designed scaffolds were docked using the aforesaid softwares keeping all the parameters same as described earlier. The docking scores of scaffolds are tabulated in table 2 (supporting information).

2.2. Synthetic Methodology

General Methods

All the reactions except hydrolysis were carried out under Nitrogen atmosphere using dried, nitrogen-purged glasswares and dry solvents. Reaction progress was monitored using Merck TLC Silica gel 60 F_{254} plates. The plates were visualized using 254 nm UV light, Iodine chamber and Ninhydrin dip where appropriate followed by gentle warming. Solvents were evaporated using Büchi rotary evaporator. Further drying was facilitated by using high vacuum. For column chromatography, silica gel (100-200 mesh) was used. IR spectra were recorded on thermo Nicolate spectrophotometer and only selected absorbances are quoted as √ in cm^{-1}. NMR spectra were run in DMSO-d_6 or $CDCl_3$ and recorded at 400 MHz on Bruker 400 MHz FTNMR Avance-III. The following abbreviations are used for the description of NMR spectra: s- singlet; bs- broad singlet; d- doublet; t- triplet; q- quartet; dd- doublet of doublets and m- multiplet. Mass spectra were recorded on LCMS Agilent 6320 Ion Trap. Preparative HPLC were done on Gilson-binary gradient auto purification system. HPLC were recorded on Agilent 1290 ultrahigh performance LC DAD using the columns Zobrax Eclipse plus C18, 50 X 2.1 mm, 1.8 µ or ACQUITY BEH C18, 50 × 2.1 mm, 1.7 µ; and the injection volumes varied from 0.5- 3.0 µl. The mobile phase used for HPLC was H_2O: CH_3CN + 0.1 % NH_4OH or Formic acid. Melting points were recorded in open capillaries using DBK melting point apparatus and were uncorrected.

3. RESULTS AND DISCUSSION

3.1. Molecular Modeling Studies

3.1.1. Analysis of crystal structures of JNK1

After analyzing the crystal structure of JNK1 it was observed that the pepJIP1 binding site on JNK1 is very well defined and is near the ATP binding site (Figure 13). As reported earlier by Heo, Y. S.; *et al*. *EMBO*. **2004**., pepJIP1 is an allosteric inhibitor of JNK1 and scaffold mimics of pepJIP1 could serve as very efficient allosteric inhibitors of JNK1 [30]. This binding site was taken as a site for the design of compounds as allosteric inhibitors of JNK1. The complex JNK1-pepJIP1 shows that the backbone amide of Leu160 of pepJIP1 hydrogen bonds with the backbone carbonyl of Ser161 of JNK1. The oxygen atom of the backbone carbonyl of Thr159 makes a hydrogen bond with the N^{ε} atom of Arg127. And Arg156 forms a bidentate salt bridge with Glu329. All these interactions are shown in Figure 14.

Also it is shown that site directed mutagenesis of Arg127 and Glu329 changes the binding constant significantly (Table 1) of pepJIP1-JNK1 complex formation, signifying the role of these resides in binding [30]. It suggests that bridging these two residues which small molecules can potentially inhibit the binding of pepJIP1to JNK1.

Table 1| Binding constant (Kd) for the JNK1-pepJIP1 binding

Protein	**Kd for pepJIP1 binding to the respective proteins (µM)**
Wild type	0.42 ± 0.13
R127A	6.4 ± 2.2
E329A	9.1 ± 3.4

[R127A and E329A are the mutants of JNK1 in which Arg127 and Glu329 were replaced by Alanine respectively].

3.1.2. Docking studies of reported JNK1 allosteric inhibitors

The docking studies of reported JNK1 allosteric inhibitors confirmed that Arg127 and Glu329 of JNK1 are the critical residues for binding to its scaffold protein JIP1 which could be targeted to design efficient allosteric inhibitor. It is been reported by Stebbins, J. L.; *et al*. *Proc. Natl. Acad. Sci*. **2008**.; that Cys163 of JNK1 also has some contribution in the binding of pepJIP1 competitive BI-78D3 which is reported as JNK1 allosteric inhibitor. The role of Arg127 and Cys163 of JNK1 was confirmed using ITC experiments where free energy of binding (ΔG) of BI-78D3 to the wild type construct of JNK2 was compared with the mutants JNK1 R127A and C163S (JNK2 amino acid numbering is the same). The reduction in the dissociation constant (Table 2) of BI-78D3 for the R127A and C163S as compared with the wild type construct shows the involvement of Arg127 and Cys163 in binding to BI-78D3 [31].

However in the present studies the importance Cys163 could not be determined as the docking poses of reported compounds failed to pick up any such interaction. The overall geometry of the pocket did not favor binding of Cys163 with the inhibitors when docked with any of the three softwares. This might be due to the low binding affinity of the compounds in that region.

Table 2| Binding constant (Kd) for the BI-78D3 binding

Protein	**Kd for BI-78D3 binding to the respective proteins (μM)**
Wild type	8.1 ± 3.8
R127A	14.7 ± 7.5
C163S	51.1 ± 11.9

It is also predicted that benzodioxan moiety of BI-78D3 occupies the region corresponding to Leucines of pepJIP1. Also an extensive network of hydrogen bonding interactions between BI-78D3 and the thiazole, triazole and nitro group of BI-78D3 (Figure 16) [31]. All these interactions were seen in the docking studies (Figure 17).

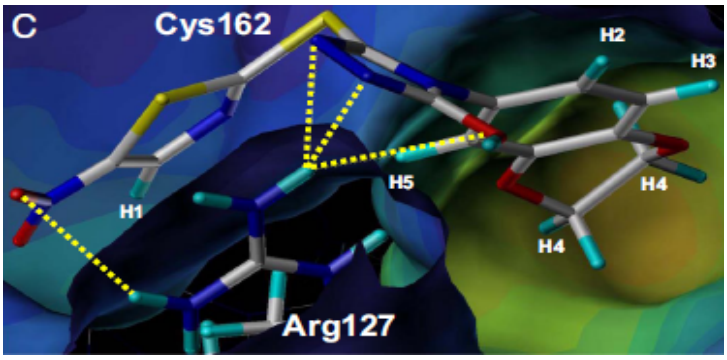

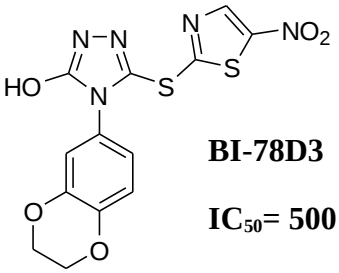

BI-78D3

IC_{50}= 500 nM

Figure 16| Docked structure of BI-78D3 into the crystal structure of JNK1 (PDB ID- 1UKI) [31]

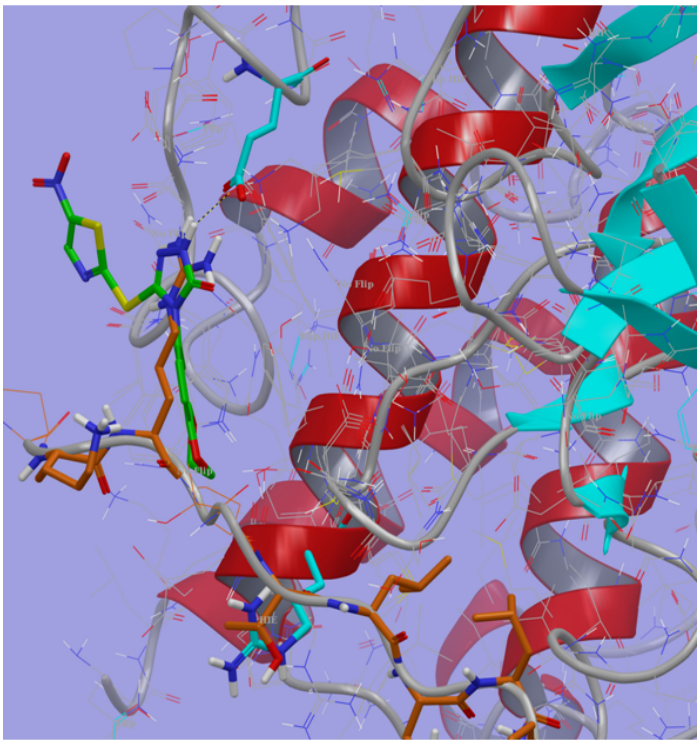

Figure 17| Docking pose of BI-78D3 generated using GLIDE.

3.1.3. Design of allosteric inhibitors

After identifying the critical residues of JNK1-pepJIP complex, the structural mimics of the pepJIP1 residues were designed which would interact with the hot spots of JNK1. The docking of the reported JNK1 inhibitors was useful in the design process since it identified the functional groups which interact with the key residues (Arg127 & Glu329) quite efficiently. Based on this 69 compounds were designed by iterative docking process. In each iteration of docking process the functional groups were modified in order to get the higher *in silico* binding affinity and the best geometrical fit with respect to pepJIP1. The geometrical fit was analyzed by molecular overlay of the docked poses on the native pepJIP1-JNK1 complex. The result of each docking phase and the rational for modification is described below and all the docking scores are tabulated in table 2 (supporting information).

The compound **23** was chosen as first promising compound from modeling perspective since it exhibited the most appropriate and persuading geometry fit (Figure 4) as compared to the other compounds.

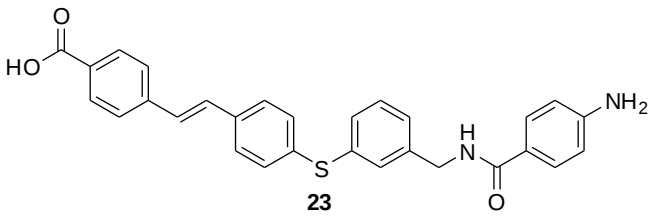

23

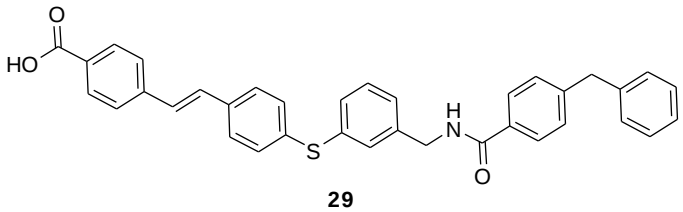

29

This compound was further modified to different analogs to optimize the binding geometry. The terminal amino group of **23** was modified to get even better overlap with pepJIP1. The right region of pepJIP1 is hydrophobic (Leu162 and Phe163) where phenylamine of **23** cannot fit. So the aniline of **23** was replaced with hydrophobic moieties like diphenylmethane, 1, 1'-biphenyl, (trichloromethyl)benzene, ethoxybenzene and 2-methylnaphthalene.

Among these diphenylmethane derivative (**29**) gave the best docking result which was inferred from the following observations.

1. Unlike other structures all the docking poses of **29** were intact around the pepJIP1 binding region.
2. The distance between Glu329 and **23** was 10.3 Å which is just 2.4 Å in **29** (figure 18.1 and 18.2) which lead to the formation of H-bond between Glu329 and **29**.
3. The docking scores of **29** is higher than **23** (table 2, supporting information).

The docking poses of **29** showed that the 4' double bond was causing the rigidity around m-tolyl(4-vinylphenyl)sulfane (A). This rigidity troubled **29** to effectively cross the bridge between Glu329 and Arg127 with a good geometric fit. To make it flexible and get a better crossing substructure we modified **29** around m-tolyl(4-vinylphenyl)sulfane (A) to get **39** which exhibited a good geometrical fit excellent shielding of pepJIP1 (figure 18.3). But the lower docking score of **39** and challenges involved in the synthesis of tricyclic phenoxanthiine (B) derivatives caused its further modification around phenoxanthiine ring.

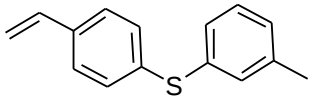

m-tolyl(4-vinylphenyl)sulfane
(A)

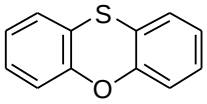

phenoxanthiine
(B)

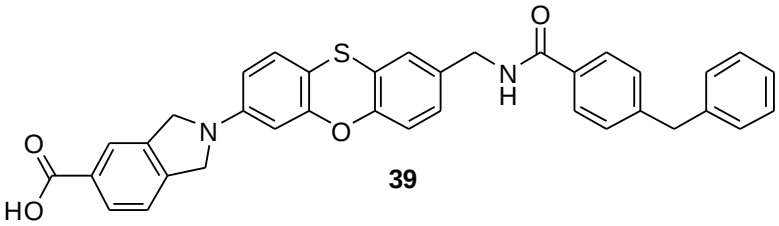

39

In this modification **47** showed the potential of highest binding affinity (table 2- supporting information) and a fair geometrical fit mimicking pepJIP1 at the appropriate places (Figure 18.4). Docking poses of **47** showed that diphenylmethane was floating freely which was then further modified to get **53**.

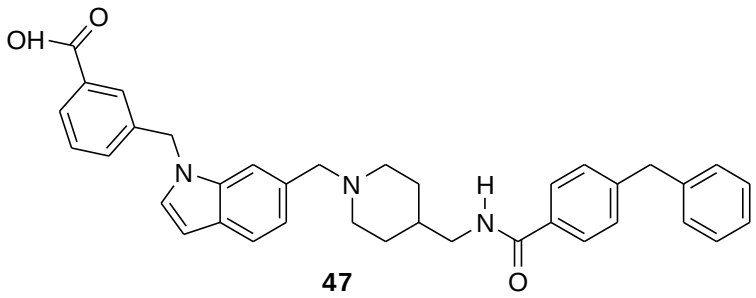

47

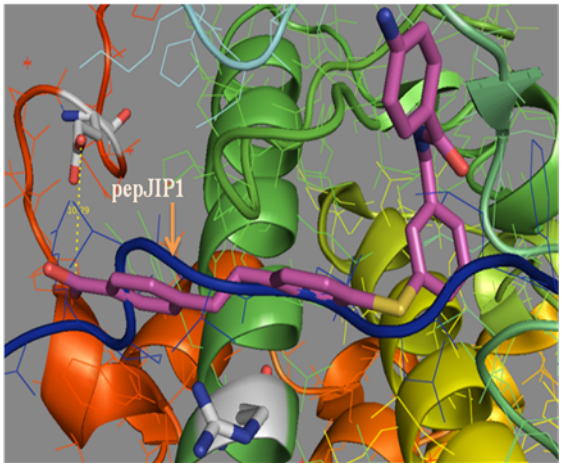

Figure 18.1| Docking pose of **23**

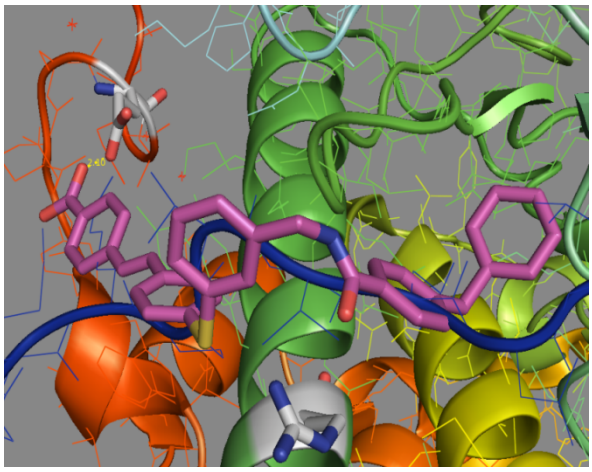

Figure 18.2| Docking pose of **29**

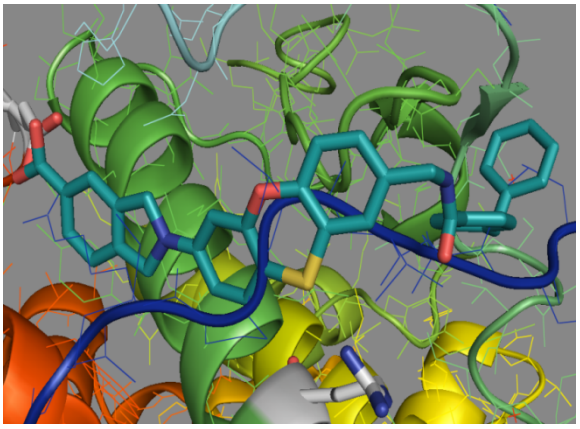

Figure 18.3| Docking pose of **39**

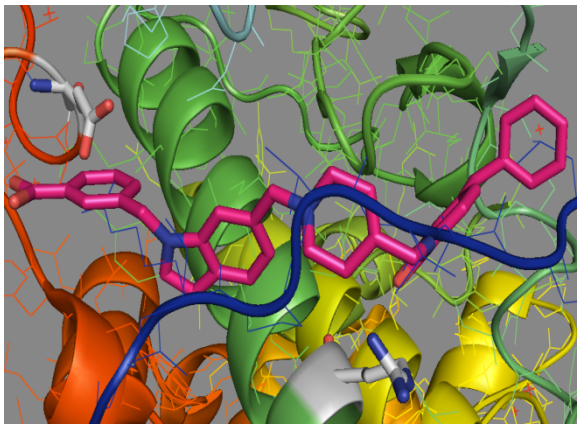

Figure 18.4| Docking pose of **47**

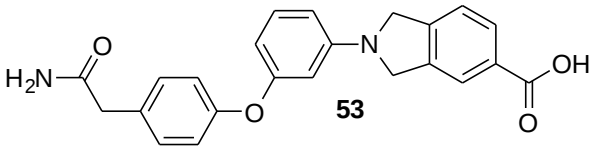

53

Docking poses of **53** showed that it blocks the interactions between pepJIP1Arg156 and JNK1Glu329 which is very crucial for binding of pepJIP1. Also free N-H forms an H-bond with Glu329 at the distance 1.86Å while pepJIP1 lies at 3.2Å from Glu329 (figure 18.5 and 18.6). This means the strength of H-bonding between **53** and Glu329 is greater as compared to pepJIP1 which would be a crucial factor in terms of binding affinity of **53**.

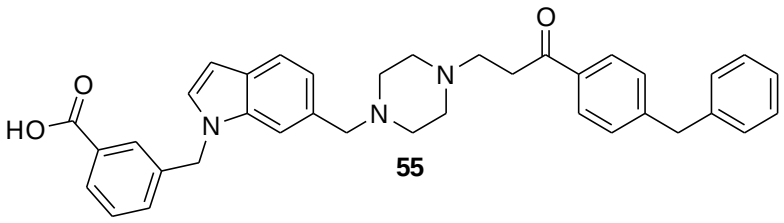

55

Similarly docking pose of **55** showed the most appropriate docking pose with respect to the geometry of pepJIP1. But it did not form any H-bond with JNK1; also the acid group of JNK1Glu329 is in close proximity to the nonpolar diphenylmethane of **55** which consequently exhibited the lower docking scores of **55**. This nonpolar group was further modified into polar group in order to increase the binding affinity. It was substituted with 2-phenylacetamide (**68**) and benzamide (**69**) derivatives in order to enhance binding affinity.

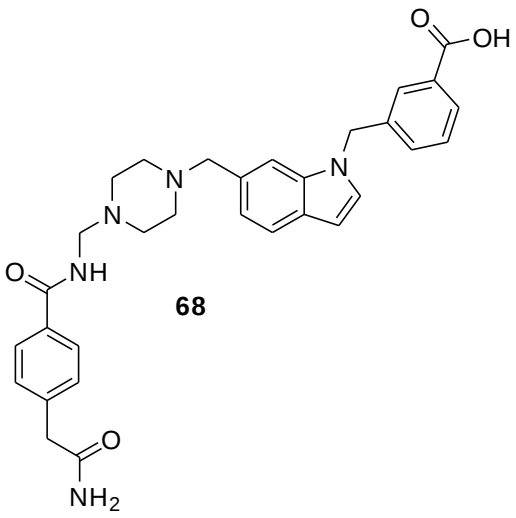

68

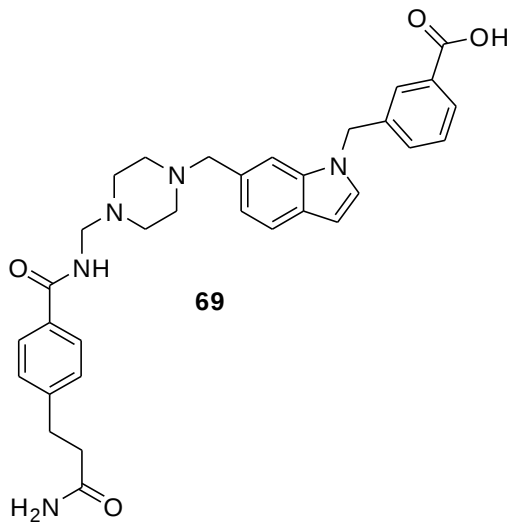

69

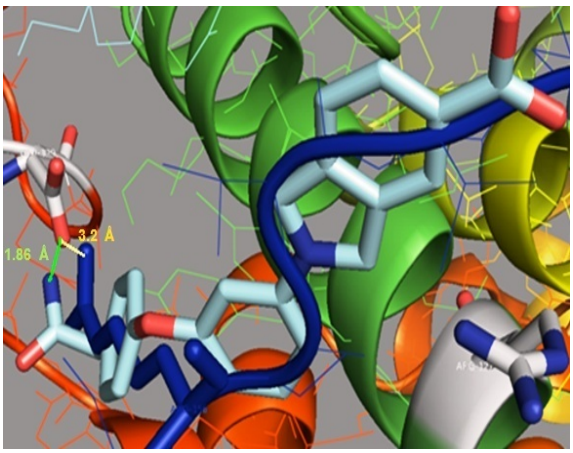

Figure 18.5| Docking pose of **53**

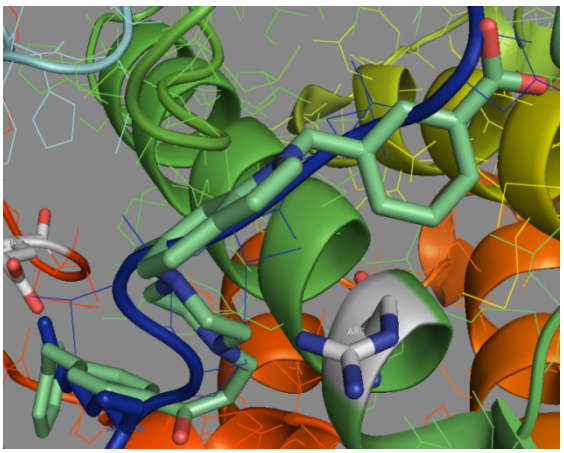

Figure 18.6|Docking pose of **55**

68 formed the H-bond with Arg127 with unexpected twisting (figure 18.7). But **69** displayed H-bond to Glu329, higher scores and a great geometrical fit perturbing the crucial JNK1Glu329-pepJIPArg156 and JNK1Arg127-pepJIPThr329 interactions (figure 18.8). But the synthetic complexity of these benzamide derivatives kept it on hold for its synthesis.

61 turned up as a promising scaffold blocking pepJIP1Arg156 and JNK1Glu329 critical interaction and forming H-bond with Arg127 as compared to the pepJIP1Thr159 (figure 18.9). It leads to the efficient interaction of **61** with Arg127 as compared to pepJIP1Thr159.

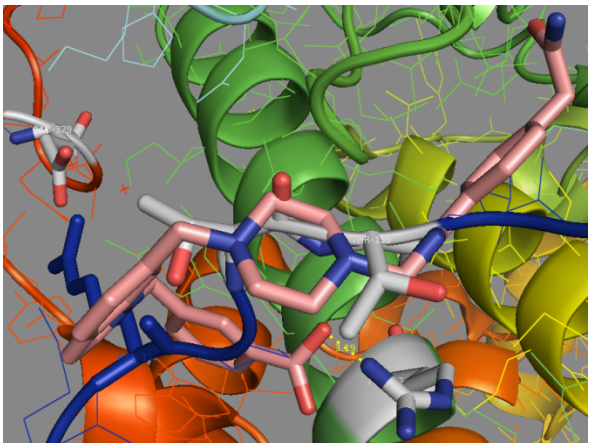

Figure 18.7| Docking pose of **68**

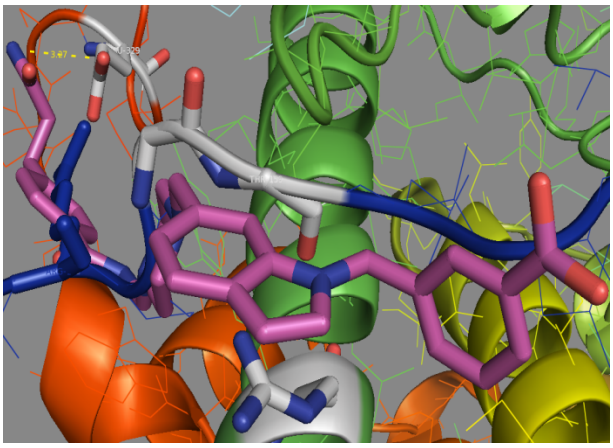

Figure 18.8| Docking pose of **69**

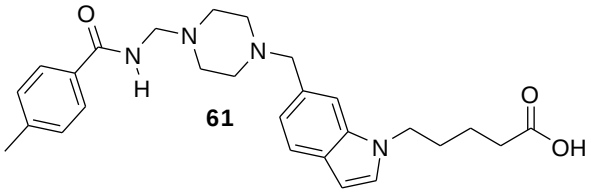

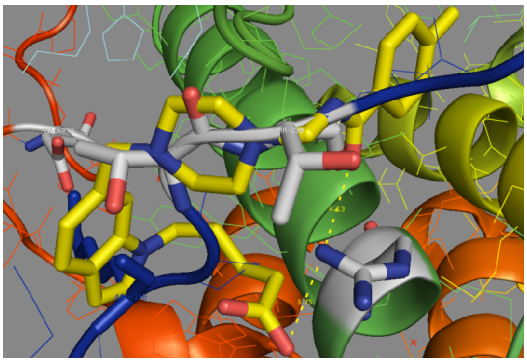

Figure 18.9| Docking pose of **61**

Based on the synthetic feasibility of the scaffold **61**, the following compounds were modified by iterative docking and synthesized. The docking poses of all the synthesized compounds show that they geometrically mimic pepJIP1 and bind around the crucial residue Arg127 of JNK1 (figure 19). The aromatic region of the compounds enters into the hydrophobic pocket of JNK1 and oxygen of the carbonyl forming hydrogen bond with the Ser128 of JNK1.

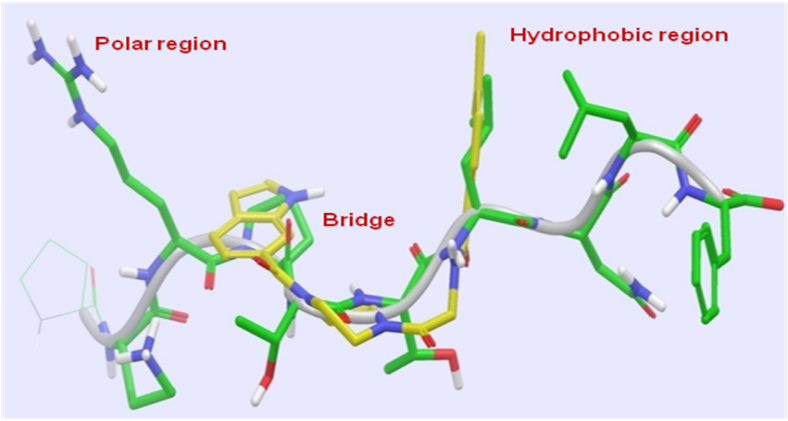

Figure 19| Implication of design strategy

The final compounds (yellow color) bind to pepJIP1 (green color) binding site which was desirable.

Table 3| Synthesized designed compounds

Compound	Structure	IUPAC Name
1	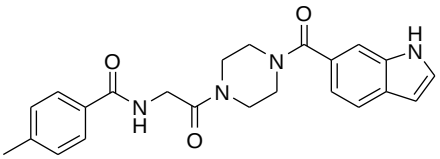	N-(2-(4-(1H-indole-6-carbonyl)piperazin-1-yl)-2-oxoethyl)-4-methylbenzamide
2	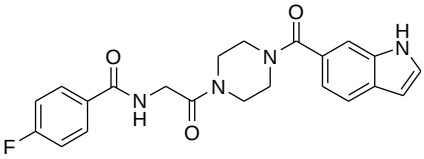	N-(2-(4-(1H-indole-6-carbonyl)piperazin-1-yl)-2-oxoethyl)-4-fluorobenzamide
3	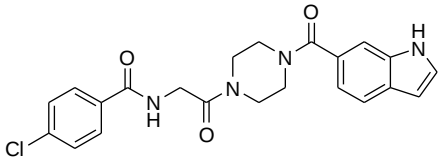	N-(2-(4-(1H-indole-6-carbonyl)piperazin-1-yl)-2-oxoethyl)-4-chlorobenzamide
4	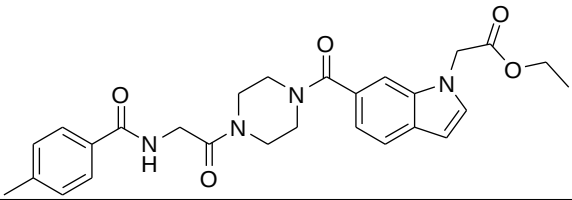	ethyl 2-(6-(4-(2-(4-methylbenzamido)acetyl)piperazine-1-carbonyl)-1H-indol-1-yl)acetate
5	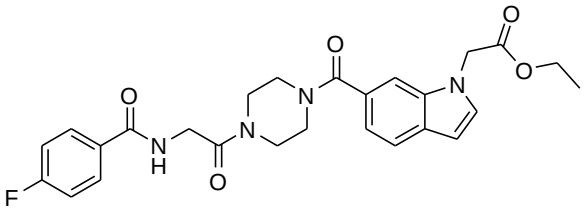	ethyl 2-(6-(4-(2-(4-fluorobenzamido)acetyl)piperazine-1-carbonyl)-1H-indol-1-yl)acetate
6	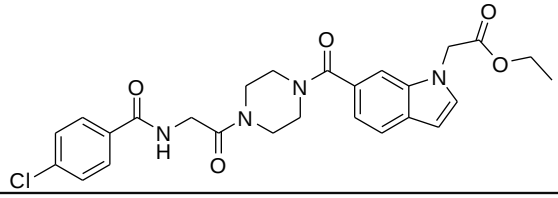	ethyl 2-(6-(4-(2-(4-chlorobenzamido)acetyl)piperazine-1-carbonyl)-1H-indol-1-yl)acetate

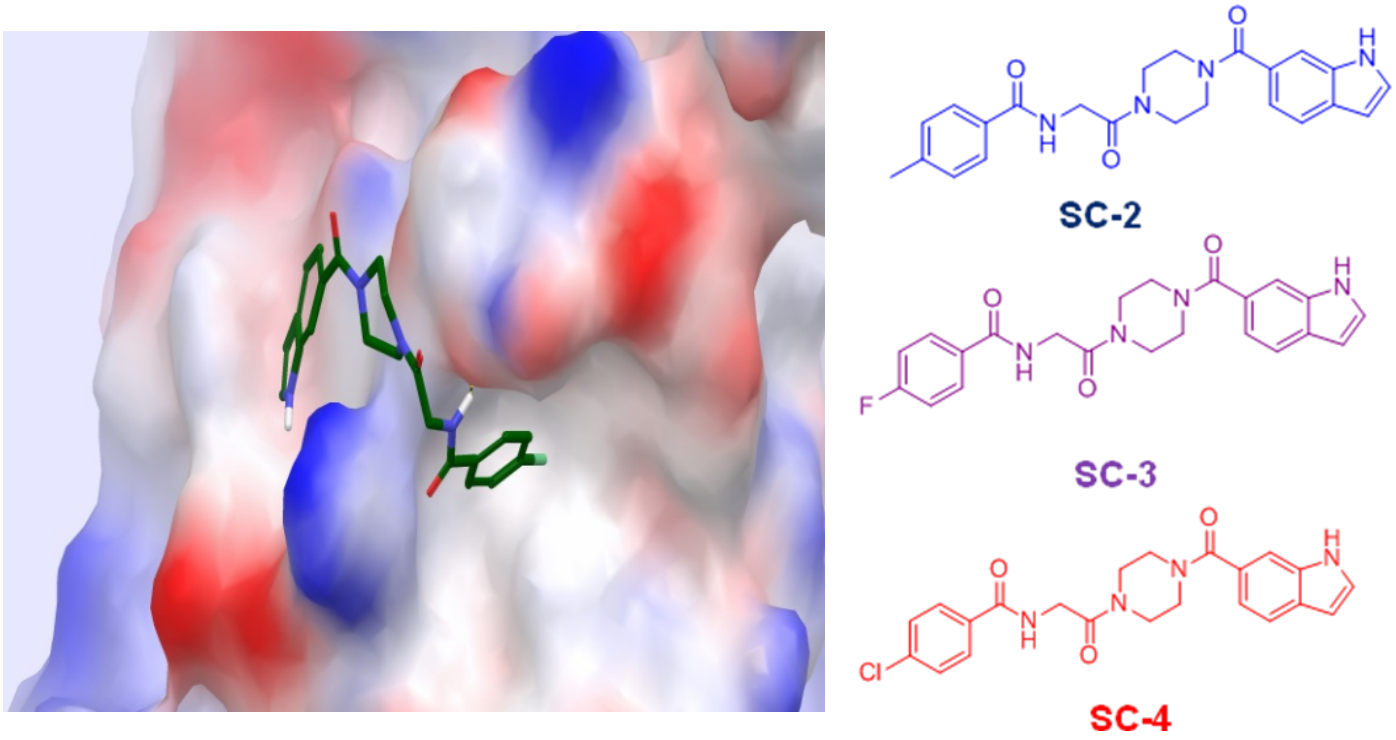

Figure 20.1| Representative docking pose of the synthesized compounds (SC-2 to SC-4)

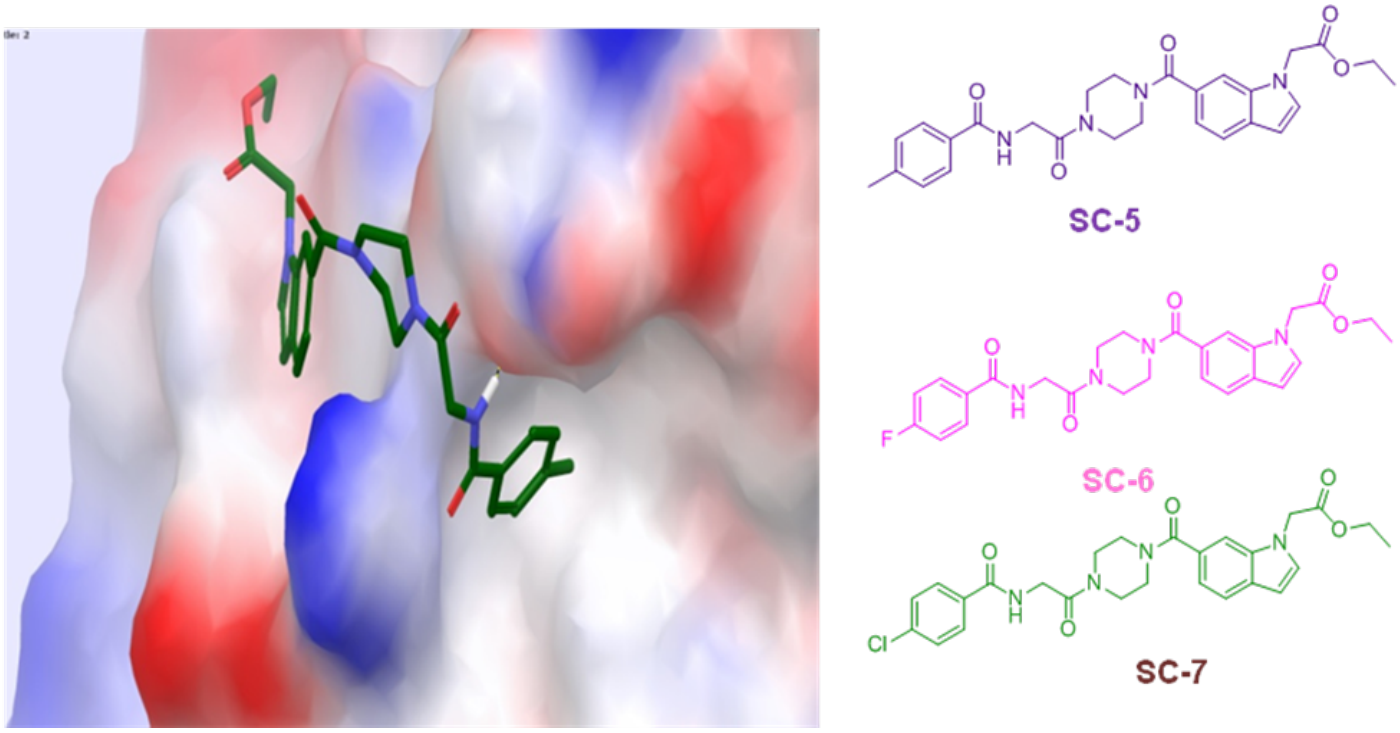

Figure 20.2| Representative docking pose of the synthesized compounds (SC-5 to SC-7)

3.2. Synthesis of compounds

3.2.1. Synthesis of standard compound

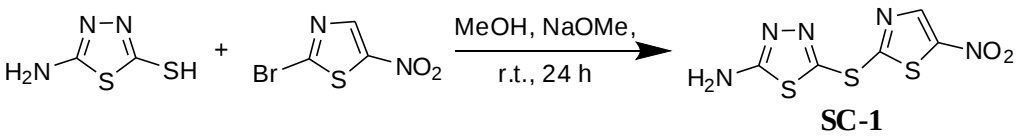

SC-1

Scheme 1: Synthesis of standard compound

Procedures

Preparation of 5-((5-nitrothiazol-2-yl)thio)-1,3,4-thiadiazol-2-amine:

To a stirred solution of 5-amino-1,3,4-thiadiazole-2-thiol (500 mg, 3.753 mmol) in MeOH (12 ml) was added NaOMe (300 mg, 5.555 mmol) and stirred at RT under N_2 atmosphere. After 10 min, 2-bromo-5-nitrothiazole (784 mg, 3.753 mmol) was added to the reaction mixture and stirred at RT for 24 h. The reaction mixture was then acidified with 1 N HCl and the pH was adjusted to 1-2. The resulting precipitate was filtered and washed with water (3 × 40 mL), hexanes (3 × 40 mL) and 5% ethyl acetate in hexanes (3 × 40 mL) to give a brown solid. The residue was chromatoghaphed over silica gel (65 % ethyl acetate in hexanes) to afford the desired product (245 mg, 25%).

HPLC Purity- 98.87%; ^{1}H NMR (400 MHz, DMSO-d_6) δ 7.96 (s, 2H), 8.76 (s, 1H); MS *m/z* 261.9 $(M + H)^+$, 293.9 $(M + Na)^+$; IR (cm^{-1}) 3270, 3065, 1637, 1344, 1140, 1042, 816,731; Melting Point- 173- 175 °C.

3.2.2. Synthesis of allosteric inhibitors

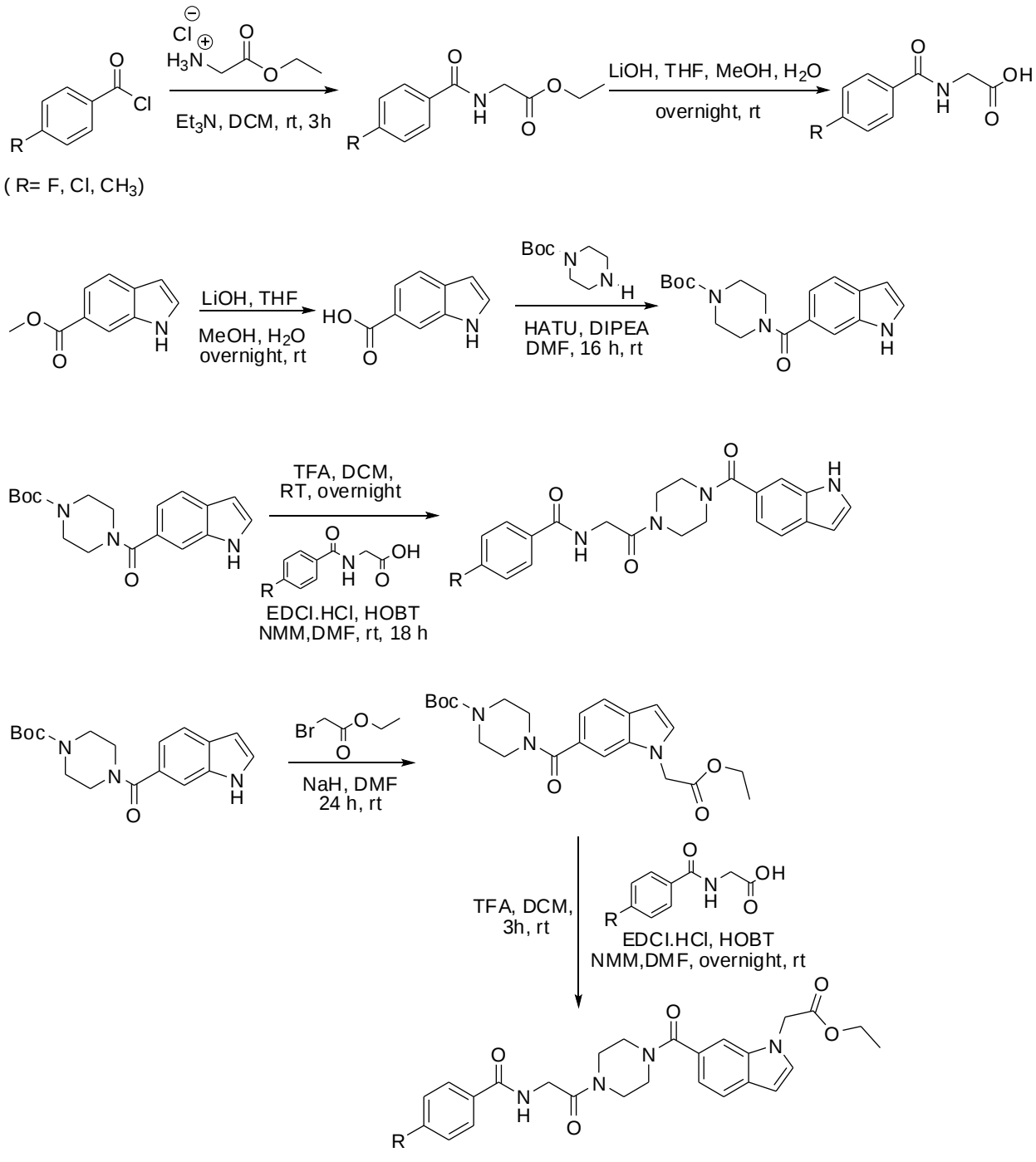

Scheme 2| General Scheme for the synthesis of designed compounds

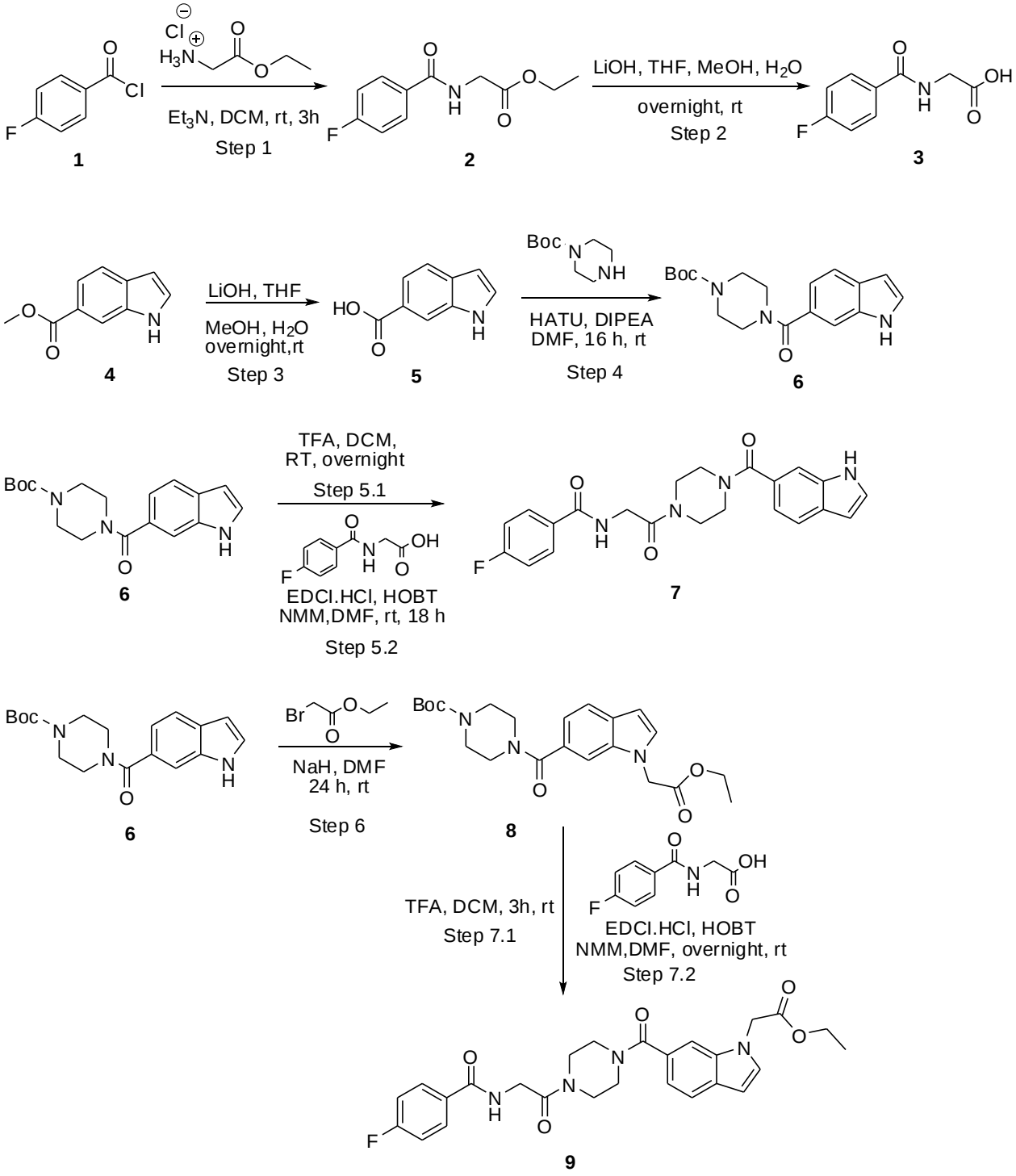

Scheme 3| Representative Scheme for the synthesis of designed compounds

Procedures

Preparation of ethyl 2-(6-(4-(2-(4-fluorobenzamido)acetyl)piperazine-1-carbonyl)-1H-indol-1-yl)acetate (10)

Step 1: Preparation of ethyl 2-(4-fluorobenzamido)acetate (2)

To a stirred solution of ethyl 2-aminoacetate hydrochloride (7.04 g, 50. 46 mmol) in DCM (20 ml) was added Et_3N (14.4 ml, 101 mmol) dropwise and the reaction mixture was stirred at RT under N_2 atmosphere. After 10 min period 4-fluorobenzoyl chloride (3 ml, 25.23 mmol) was added dropwise at 0°C and the reaction mixture was stirred at RT for 3 h. The solvents were then evaporated under reduced pressure and the resulting brown solid was washed with water (3 × 50 ml), extracted in ethyl acetate (4 × 50 ml) and dried over Na_2SO_4 to get the crude product which was then purified using column chromatography (45% EtOAc in hexane) to get the desired product as a pale yellow solid (4.8 g, 84.5%).

^{1}H NMR (400 MHz, DMSO-d_6) δ 1.2 (t, 3H, J= 7 Hz), 2.08 (s, 1H), 3.99 (d, 2H, J= 6 Hz), 4.11 (q, 2H), 7.33 (m, 2H), 7.93 (m, 2H), 8.98 (t, 1H, J= 11 Hz); MS *m/z* 226.1 $(M + H)^+$, 248.1 $(M + Na)^+$.

Step 2: Preparation of 2-(4-fluorobenzamido)acetic acid (3)

To a stirred solution of ethyl 2-(4-fluorobenzamido)acetate (**2)** (2.8 g, 12.43 mmol) in THF (15 ml); LiOH (2.6 g, 62.15 mmol) in H_2O (15 ml); MeOH (2-3drops) were added and the reaction mixture was stirred at RT for overnight. After that solvents were evaporated under the reduced pressure. The reaction mixture was acidified by 2 N HCl solution (pH= 1-2) at 0°C and the resulting precipitate was filtered to afford the white solid (2.34 g, 95.5%) which was used further without any purification.

HPLC Purity- 92.79%; ^{1}H NMR (400 MHz, DMSO-d_6) δ 3.91 (d, 2H, J= 6 Hz), 7.32 (m, 2H), 7.95 (m, 2H), 8.88 (t, 1H, J=12 Hz), 12.63 (s, 1H); MS *m/z* 198.0 $(M + H)^+$, 220.0 $(M + Na)^+$.

Step 3: Preparation of 1*H*-indole-6-carboxylic acid (5)

To a stirred solution of methyl 1*H*-indole-6-carboxylate (**4**) (6 g, 34.25 mmol) in THF (25 ml), LiOH (7.2 g, 171.2 mmol) in H_2O (25 ml), MeOH (4-5 drops) were added and the reaction mixture was stirred at RT for overnight. After that the solvents were evaporated under the reduced pressure. The reaction mixture was acidified by 2 N HCl solution (pH= 1-2) at 0°C and the resulting precipitate was filtered to afford the brown solid (4.5 g, 82%) which was used further without any purification.

HPLC Purity- 95.27%; ^{1}H NMR (400 MHz, DMSO-d_6) δ 6.5 (m, 1H), 7.59 (m, 3H), 8.04 (m, 1H), 11.5 (d, 1H, J= 20 Hz), 12.50 (s, 1H); MS *m/z* 162.1 $(M + H)^+$.

Step 4: Preparation of tert-butyl 4-(1H-indole-6-carbonyl)piperazine-1-carboxylate (6)

To a stirred solution of 1*H*-indole-6-carboxylic acid (**5**) (870 mg, 5.4 mmol) in DMF (10 ml) was added HATU (4.1 g, 10.8 mmol), tert-butyl piperazine-1-carboxylate (1.5 g, 8.1 mmol) and DIPEA (3.0 ml, 21.6 mmol) under N_2 atmosphere. The reaction mixture was then stirred at RT for 16 h. After that the reaction mixture was quenched with ice water and extracted in EtOAc (3 × 50 ml) and dried over Na_2SO_4 to get the brown colored crude which was then purified using column chromatography (60% EtOAc in hexane) to afford the pale brown solid (1.3 g, 73%).

^{1}H NMR (400 MHz, $CDCl_3$) δ1.46 (s, 9H), 3.44 (bs, 8H), 6.51 (m, 1H), 7.06 (dd, 1H, J= 9.6 Hz), 7.29 (m, 2H), 7.43 (s, 1H), 7.55 (m, 1H), 9.18 (s, 1H); MS *m/z* 330.3 $(M + H)^+$, 352.3 $(M + Na)^+$.

Step 5: Preparation of *N*-(2-(4-(1H-indole-6-carbonyl)piperazin-1-yl)-2-oxoethyl)-4-fluorobenzamide (7)

Step 5.1: To a stirred solution of tert-butyl 4-(1H-indole-6-carbonyl)piperazine-1-carboxylate (625 mg, 1.91 mmol) (**6**) in DCM (8 ml) was added TFA (8 ml) at 0°C under N_2 atmosphere and the reaction mixture was warmed to RT and stirred for overnight. After that the solvents were evaporated under reduced pressure and the resulting brown semisolid was treated with toluene (2 × 20 ml) and dried under vacuum to get the brown semisolid which was used further without any purification and characterization.

Step 5.2: To a stirred solution of TFA salt of tert-butyl 4-(1H-indole-6-carbonyl)piperazine-1-carboxylate (625 mg, 1.91 mmol) in DMF (5 ml) was added HOBT (470 mg, 3.1 mmol), 2-(4-fluorobenzamido)acetic acid (**3**) (300 mg, 1.5 mmol), NMM (2 ml) and EDCI.HCl (600 mg, 3.1 mmol) under N_2 atmosphere and the reaction mixture was stirred for 18 h. After that reaction was quenched by cold water and stirred for 20 min at RT. The resulting precipitate was filtered and purified using column chromatography (4% MeOH in DCM) followed by preparative HPLC to afford the white solid (140 mg, 23 %).

HPLC Purity-92.33 %; ^{1}H NMR (400 MHz, DMSO-d_6): δ 3.34 (m, 8H), 4.15 (d, 2H, J= 4.8 Hz), 7.04 (dd, 1H, J= 8.4 Hz), 7.15 (d, 1H, J= 2.4 Hz), 7.3 (t, 2H, J= 17.6 Hz), 7.44 (s, 1H), 7.74 (d, 1H, J= 8.4 Hz), 7.93 (q, 2H), 8.64 (t, 1H, J=10.8 Hz); MS *m/z* 409.3 $(M + H)^+$, 431.2 2$(M + Na)^+$; Melting Point: 295 °C.

Step 6: Preparation of tert-butyl 4-(1-(2-ethoxy-2-oxoethyl)-1H-indole-6-carbonyl)piperazine-1-carboxylate (8)

To a stirred solution of tert-butyl 4-(1H-indole-6-carbonyl)piperazine-1-carboxylate (**6**) (800 mg, 2.43 mmol) in DMF (5 ml) was added NaH (60%, 90 mg, 3.65 mmol) at 0°C under N_2 atmosphere and the reaction mixture was stirred at RT. After 1 h, ethyl 2-bromoacetate (820 mg, 4.87 mmol) was added to the reaction mixture at 0°C and the reaction mixture warmed to RT and stirred for 24 h. After that reaction was quenched by ice, stirred for 20 min, extracted in EtOAc (3× 50 ml) and dried over Na_2SO_4 to get the brown solid which chromatographed over silica gel (60% EtOAc/ hexane) to afford the pale yellow solid (900 mg, 89%).

HPLC Purity- 96.12 %; ^{1}H NMR (400 MHz, DMSO-d_6): δ 1.25 (t, 3H, J= 12 Hz), 1.45 (s, 9H), 3.44 (bs, 8H), 4.20 (q, 2H, J= 4 Hz), 4.84 (s, 2H), 6.56 (s, 1H), 7.12 (dd, 1H, J= 4 Hz), 7.17 (d, 1H, J= 4 Hz), 7.39 (s, 1H), 7.6 (d, 1H J=8 Hz), MS *m/z* 416.2 $(M + H)^+$, 438.2 $(M + Na)^+$.

Step 7: ethyl 2-(6-(4-(2-(4-fluorobenzamido)acetyl)piperazine-1-carbonyl)-1H-indol-1-yl)acetate (9)

Step 7.1: To a stirred solution of tert-butyl 4-(1-(2-ethoxy-2-oxoethyl)-1H-indole-6-carbonyl)piperazine-1-carboxylate (**6**) (750 mg, 1.75 mmol) in DCM (6 ml) was added TFA (6

ml) at 0°C under N_2 atmosphere and the reaction mixture was warmed to rt and stirred for overnight. After that the solvents were evaporated under reduced pressure and the resulting brown semisolid was treated with toluene and dried under vacuum to get the brown semisolid which was used further without any purification and characterization.

Step 7.2: To a stirred solution of TFA salt of tert-butyl 4-(1-(2-ethoxy-2-oxoethyl)-1H-indole-6-carbonyl)piperazine-1-carboxylate (750 mg, 1.75 mmol) in DMF (5 ml) was added HOBT (540 mg, 3.5 mmol), 2-(4-fluorobenzamido)acetic acid (**3**) (230 mg, 1.2 mmol), NMM (2 ml) and EDCI.HCl (670 mg, 3.5 mmol) under N_2 atmosphere and the reaction mixture was stirred for 18 h. After that ice was added to the reaction mixture and stirred for 20 min at RT. The resulting precipitate was filtered and purified using column chromatography (5% MeOH in DCM) followed by preparative HPLC to afford the white solid (30 mg, 5%).

HPLC Purity- 89.08 %; ^{1}H NMR (400 MHz, $CDCl_3$): δ 1.21 (t, 3H J=14 Hz), 3.55 (m, 8H), 4.15 (m, 4H), 5.18 (s, 2H), 6.53 (d, 1H, J= 4 Hz), 7.1 (dd, 1H J=4 Hz), 7.45 (m, 1H), 7.55 (m, 3H), 7.61 (m, 1H), 7.48 (dd, 2H, J= 4 Hz), 8.7 (t, 1H J=12 Hz); MS *m/z* 511.1 $(M + H)^+$, 533.1 $(M + Na)^+$, Melting Point- 93 °C.

Intermediates

The following intermediates were synthesized in the preparation of final compounds.

Table 4| Characterization data of the intermediates (scheme 2)

SN	Structure	IUPAC name	^{1}H NMR (400 MHz)	Mass $(M+H)^+$
1	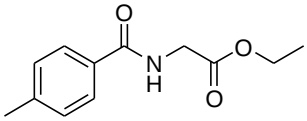	ethyl 2-(4-methylbenzamido)acetate	DMSO-d_6, δ 1.2 (t, 3H, J= 14 Hz), 2.36 (s, 3H), 3.97 (d, 2H, J= 6 Hz), 4.11 (q, 2H, J= 21.6), 7.28 (d, 2H, J= 7.6 Hz), 7.78 (m, 2H), 8.85 (t, 2H, J= 11.6 Hz)	222.1
2	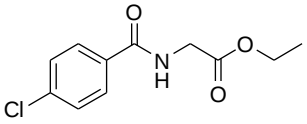	ethyl 2-(4-chlorobenzamido)acetate	$CDCl_3$, δ 1.34 (m, 3H), 4.27 (m, 4H), 6.63 (s, 1H), 7.43 (m, 2H), 1.77 (m, 2H)	242.0
3	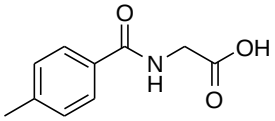	2-(4-methylbenzamido)acetic acid	DMSO-d_6, δ 2.50 (m, 3H), 3.90 (d, 2H, J= 6 Hz), 7.28 (m, 2H), 7.78 (m, 2H), 8.76 (t, 1H, J= 12 Hz), 12.59 (bs, 1H)	194.0
4	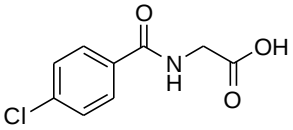	2-(4-chlorobenzamido)acetic acid	DMSO-d_6, δ 3.92 (d, 2H, J= 5.6 Hz), 7.56 (m, 2H), 7.91 (m, 2H), 8.94 (t, 1H, J= 11.6 Hz), 12.71 (bs, 1H)	213.9

Final Compounds

Table 5| Characterization data of final compounds of scheme 2

SN	Structure	IUPAC name	^{1}H NMR (400 MHz)	Mass	HPLC	MP (°C)
1	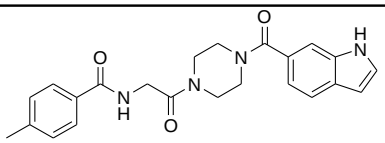	N-(2-(4-(1H-indole-6-carbonyl)piperazin-1-yl)-2-oxoethyl)-4-methylbenzamide	DMSO-d_6, δ 2.5 (s, 1H), 3.5 (bs, 8H), 4.14 (d, 2H, J= 5.6), 6.49 (m, 1H), 7.07 (dd, 1H, J= 8.4 Hz), 7.28 (d, 2H, J= 8 Hz), 7.47 (m, 2H), 7.59 (d, 1H, J= 8.4 Hz), 7.77 (d, 2H, J= 8Hz), 8.51 (t, 1H, J= 11.2 Hz), 11.32 (s, 1H)	405.2	96.94	240
2	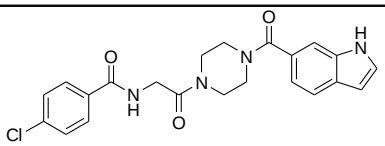	N-(2-(4-(1H-indole-6-carbonyl)piperazin-1-yl)-2-oxoethyl)-4-chlorobenzamide	DMSO-d_6+ D_2O, δ 3.56 (bs, 8H), 4.14 (s, 2H), 6.49 (d, 1H, J= 2.8 Hz), 7.06 (d, 1H, J= 8.4 Hz), 7.46 (d, 2H, J= 3.2), 7.54 (m, 2H), 7.60 (d, 2H, J= 8.4), 7.86 (m, 2H), 8.36 (s, 1H)	425.2	99.47	343

SN	Structure	IUPAC name	^{1}H NMR (400 MHz)	Mass	HPLC	MP (°C)
3	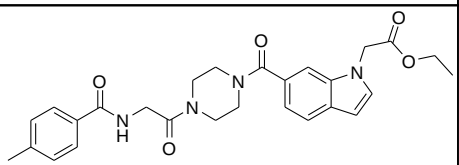	ethyl 2-(6-(4-(2-(4-methylbenzamido)acetyl)piperazine-1-carbonyl)-1H-indol-1-yl)acetate	DMSO-d_6, δ 1.19 (m, 3H), 4.03 (m, 4H), 5.19 (s, 2H), 6.53 (m, 1H), 7.12 (dd, 1H, J= 8 Hz), 7.28 (d, 2H, J= 8 Hz), 7.47 (d, 1H, J= 3.2 Hz), 7.55 (s, 1H), 7.61 (d, 1H, J= 8 Hz), 8.51 (t, 1H, J= 11.2 Hz)	491.2	92.46	95
4	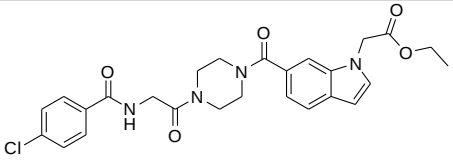	ethyl 2-(6-(4-(2-(4-chlorobenzamido)acetyl)piperazine-1-carbonyl)-1H-indol-1-yl)acetate	DMSO-d_6, δ 1.21 (t, 3H, J= 14 Hz), 3.55 (bs, 8H), 4.14 (q, 4H, J= 14.4 Hz), 5.19 (s, 2H), 6.48 (s, 1H), 7.13 (dd, 1H), J= 8 Hz), 7.46 (dd, 1H, J= 8.8 Hz), 7.565 (m, 3H), 7.61 (d, 1H, J= 8 Hz), 7.89 (m, 2H), 8.72 (t, 1H, J= 11.2 Hz)	511.1	89.08	95

4. BIOLOGICAL EVALUATION

The compounds were sent to Millipore UK for checking biological activity. The activity of each of the compounds was checked at three different concentrations (1µM, 5µM and 10µM) expecting that these compounds would inhibit the phosphorylation of JNK1 substrate. None of the synthesized compounds including the standard compound **SC1** showed any activity in a given assay condition.

Discussions are underway for refinement of the assay.

5. CONCLUSION

The small molecule allosteric inhibitors of JNK1 were designed and synthesized based on the shape/structural complementarities of the pepJIP1-JNK1 complex.

6. FUTURE PROSPECT

This project could lead to the development of JNK1 inhibitors targeting the allosteric site rather than the highly conserved ATP binding site.

BIBLIOGRAPHY

[1] Manning, G.; *et al*. The protein kinase complement of human genome. *Science*. **2002**, *298*, 1912- 1934.

[2] Bridges, A. J. Chemical Inhibitors of Protein Kinases. *Chem. Rev.* **2001**, *101*, 2541-2571.

[3] Molecular Biology of the cell, 4th edition, Garland Science (Taylor & Francis Group), New York. Alberts, B.; *et al*. **2008**.

[4] Kaidanovich-Beilin, O.; *et al*. Peptides Targeting Protein Kinases: Strategies and Implications. *Physiology*. **2006**, **21**, 411- 418.

[5] Hanks, S. K.; Hunter, T. The eukaryotic protein kinase superfamily: kinase (catalytic) domain structure and classification. *FASEB J*, **1995**, *9*, 576–596.

[6] Taylor, S. S.; *et al*. A template for the protein kinase family. *Trends Biochem Sci*. **1993**, *18*, 84- 89.

[7] Hanks, S. K.; *et al*. The protein kinase family: conserved features and deduced phylogeny of the catalytic domains. *Science*. **1988**, *241*, 42-52.

[8] Robinson, D. R.; *et al*. D. R. Robinson, Yi-Mi Wu, and Su-Fang Lin. The protein tyrosine kinase family of the human genome. Oncogene, **2000**, *19*, 5548- 5557.

[9] Araujo, R. P.; *et al*. Proteins, drug targets and the mechanisms they control: the simple truth about complex networks. *Nature Reviews Drug Discovery*. **2007**, *6*, 871- 880.

[10] Ortutay, C.; *et al*. KinMutBase: a registry of disease-causing mutations in protein kinase domains. *Hum Mutat*. **2005**, *25*, 435- 442.

[11] Cohen, P. Protein Kinases- the major drug targets of the twenty-first century. *Nature Reviews Drug Discovery*, **2002**, *1*, 309-315.

[12] Zuccotto, F.; *et al*. Through the "Gatekeeper Door": Exploiting the Active Kinase Conformation. *J. Med. Chem.* **2010,** *53*, 2681-2694.

[13] Johnson, G. L.; *et al*. Mitogen- Activated Protein Kinase Pathways Mediated by ERK, JNK and p38 Protein Kinases. *Science*, 2002, *298*, 1911- 1912.

[14] Dhanasekharan, D. N.; *et al*. Scaffold proteins of MAP-kinase modules. Oncogene. 2007, *26*, 3185- 3202.

[15] Kyriakis, J. M.; *et al*. pp54 microtubule-associated protein 2 kinase. A novel serine/threonine protein kinase regulated by phosphorylation and stimulated by poly-L-lysine. J. Biol. Chem. 1990, 265, 17355- 17363.

[16] Weston, C. R.; *et al*. The JNK signal transduction pathway. *Curr. Opi. Cell Biol*, **2007**, *19*, 142- 149.

[17] Derijard, B.; *et al*. JNK1: a protein kinase stimulated by UV light and Ha-Ras that binds and phosphorylates the c-Jun activation domain. *Cell*, **1994**, *76*, 1025–1037.

[18] Davis, R. J.; Signal transduction by the JNK group of MAP kinases. *Cell*, **2000**, *103*, 239–252.

[19] Ventura, J. J., *et al*. c-Jun NH2-terminal kinase is essential for the regulation of AP-1 by tumor necrosis factor. *Mol Cell Biol*. **2003**, *23*, 2871–2882.

[20] Bogoyevitch, M. A.; *et al*. c-Jun N-terminal kinase (JNK) signaling: recent advances and challenges. Biochim Biophys Acta. 2010, *1804*, 463- 475.

[21] Bennett, B. L.; *et al*. JNK: a new therapeutic target for diabetes. Curr Opin Pharmacol. **2003**, *3*, 420- 425.

[22] Vallerie, S. N.; *et al*. The role of JNK proteins in metabolism. *Sci Transl Med.* **2010**, *2*, 60rv5.

[23] Virkamäki A.; et al. Protein-protein interaction in insulin signaling and the molecular mechanisms of insulin resistance. *J Clin Invest*. **1999**, *103*, 931-943.

[24] Aguirre V.; *et al*. The c-Jun NH_2-terminal kinase promotes insulin resistance during association with insulin receptor substrate-1 and phosphorylation of Ser(307). *J Biol Chem*. **2000**, *275*, 9047-9054.

[25] Hirosumi J.; *et al*. A central role for JNK in obesity and insulin resistance. *Nature*, **2002**, *420*, 333-336.

[26] Bogoyevitch, M. A. Therapeutic promise of JNK ATP-noncompetitive inhibitor. *Trends in Molecular Medicine*. **2005**, *11*, 232-239.

[27] Barr, R. K.; *et al*. Identification of the critical features of a small peptide inhibitor of JNK activity. *J. Biol. Chem*. **2002**, *277*, 10987- 10997.

[28] Dickens, M.; *et al*. A cytoplasmic inhibitor of the JNK signal transduction pathway. *Science*. **1997**, *277*, 693- 696.

[29] Bonny, C.; *et al*. Cell- permeable peptide inhibitors of JNK: novel blockers of beta-cell death. *Diabetes*. **2001**, *50*, 77- 82.

[30] Heo, Y. S.; *et al*. Structural basis for the selective inhibition of JNK1 by the scaffolding protein JIP1 and SP600125. *EMBO*. **2004**, *23*, 2185- 2195.

[31] Stebbins, J. L.; *et al*. Identification of a new JNK1 inhibitor targeting JNK-JIP interaction site. *Proc Natl Acad Sci*. **2008**, *105*, 16809- 16813.

[32] Manning, M. A.; *et al*. Targeting JNK for therapeutic benefit: from Junk to Gold. *Nature Reviews*. **2003**, 2, 554- 565.

[33] Berman, H. M.; *et al*. The protein data bank. *Nucleic Acids Res*. **2000**, *28*, 235–242.

[34] Halgren, T. A.; *et al*. Glide: A new approach for rapid, accurate docking and scoring. 2. Enrichment factors in database screening. *J. Med. Chem*. **2004**, *47*, 1750–1759.

[35] Jain, A. N. Effects of protein conformation in docking: improved pose prediction through protein pocket adaptation. *J. Comput Aided Mol Design*. **2009**, *23*, 355- 374.

[36] Bastikar, V. A.; *et al*. In Silico Docking Analysis of Peptide Deformylase (PDF) - A Novel Target for Prophylaxis of Leptospirosis. *Nature Precedings*. **2008**, *6*, 21.

[37] Jorgensen. W. L.; *et al*. Potential energy functions for atomic-level simulations of water and organic and biomolecular systems. *Proc. Natl. Acad. Sci*. **2005**, *102*, 6665- 6670.

[38] Clark, M.; *et al*. Validation of the General Purpose Tripose 5.2 Force Field. *J. Comp. Chem*. **1989**, *10*, 982- 1012.

[39] Halgren, T. A. MMFF VII. Characterization of MMFF94, MMFF94s and other widely available force fields for conformational energies and for intermolecular interaction energies and geometries. *J. Comput Chem*. **1999**, 20,730–748.

[40] Gasteiger, J.; *et al*. Iterative partial equalization of orbital electronegativity—a rapid access to atomic charges. *Tetrahedron*, 1980, *36*, 3219- 3228.

[41] De. S. K.; *et al*. Design, Synthesis, and Structure-Activity Relationship of Substrate Competitive, Selective, and in Vivo Active Triazole and Thiadiazole Inhibitors of the c-Jun N-Terminal Kinase. *J. Med. Chem*. **2009**, 52, 1943–1952.

[42] Zhang, D.; *et al*. JNK1 mediates degradation HIF-1α by a VHL-independent mechanism that involves the chaperones Hsp90/Hsp70. *Cancer Res*. **2010**, *70*, 813- 823.